Tetrahedron Letters 169 (2025) 155745

Contents lists available at ScienceDirect

Tetrahedron Letters

journal homepage: www.elsevier.com/locate/tetlet

Recent progress on phenothiazine organophotoredox catalysis

Kenta Tanaka [a,*], Hiroyoshi Takamura [b], Isao Kadota [b]

[a] Research Institute for Interdisciplinary Science, Okayama University, 3-1-1 Tsushima-Naka, Kitaku, Okayama 700-8530, Japan
[b] Graduate School of Environmental, Life, Natural Science and Technology, Okayama University, 3-1-1 Tsushima-Naka, Kitaku, Okayama 700-8530, Japan

ARTICLE INFO

Keywords:
Phenothiazine
Photoredox catalysis
Visible light
Radical

ABSTRACT

Photoredox catalysis has garnered significant attention in recent years due to its broad applicability in visible-light-induced organic transformations. While significant progress has been made in the development of highly oxidizing catalysts, such as acridinium catalysts, there remains a notable shortage of strongly reducing organophotoredox catalysts. Phenothiazines are widely used as photoredox catalysts owing to their unique redox potentials, particularly their low excited-state oxidation potentials (E_{ox}^* = −1.35 V to −3.51 V vs. SCE). Thus, they can be applied to a variety of photoredox reactions with oxidative-quenching cycles, and effectively reduce various organic molecules, such as aryl and alkyl halides, alkenes, malonyl peroxides, cobalt complexes, and redox-active esters. Due to their unique properties, this review focuses on the recent advances in phenothiazine organophotoredox catalysis.

Introduction

Photoredox catalysis has attracted much attention in contemporary organic chemistry due to its utility in a wide variety of visible-light-induced organic transformations. When designing a photoredox-catalytic reaction, the redox potential of the photoredox catalyst is one of the key factors [1]. A variety of useful photoredox catalysts have been developed recently, and specifically photoredox catalysts with low excited-state oxidation potentials, which are desirable in the context of reducing a variety of electron-deficient substrates and enabling various chemical transformations via oxidative-quenching cycles, have attracted much attention [2]. While Ir-based photoredox catalysts are widely employed due to their low excited-state reduction potentials, they are fraught with the disadvantages that burden many transition-metal-based catalysts (i.e., scarcity, price, and potential toxicity). Therefore, a variety of useful metal-free organophotoredox catalysts has been developed in recent years (Fig. 1), including 4CzIPN (a), naphthochromenone (b), Eosin Y (c), phenothiazine (e), phenoxazine (f), dihydroacridine (g), and dihydrophenazine (h) [1b–c,3–6]. Typical organophotoredox catalysts are commercially available from chemical suppliers such as Sigma-Aldrich and TCI. For instance, 4CzIPN (a) costs approximately $8440/g (50 mg for $422), Eosin Y (c) $20.40/g (5 g for $102), phenothiazine (e) $860/g (100 mg for $86), phenoxazine $71/g (1 g for $71), and 5,10-dihydrophenazine $93/g (1 g for $93). Some of these organophotoredox catalysts are generally more sustainable and cost-effective compared to iridium-based catalysts such as $Ir(ppy)_3$, which costs approximately $1680/g (250 mg for $420).

Among these, phenothiazine (e) has gained particular attention as a photoredox catalyst owing to its strong reducing ability (E_{ox}^* = −2.10 V vs. SCE). Consequently, various structurally diverse phenothiazine-based catalysts with distinct redox properties have recently been developed (Figs. 2 and 3) [7–24]. Due to the electron-rich structure of phenothiazine, the *p*-position relative to the nitrogen atom is highly reactive toward electrophiles [25]. Thus, several modified phenothiazine catalysts bearing substituents at *p*-position have recently been developed (e.g. **C**, **M**, and **S**). The phenothiazine catalysts exhibit UV/Vis absorption maxima around 300 nm and fluorescence maxima around 450 nm (Fig. 4). Based on the correlation between molecular structure and excited-state oxidation potential, phenothiazine derivatives that bear electron-withdrawing substituents or π-extended frameworks such as benzo[*b*]phenothiazine exhibit high excited-state oxidation potentials (Fig. 2; **A-I**; E_{ox}^* = −1.35 V to −2.05 V vs. SCE) compared to *N*-phenyl phenothiazine (**J**; E_{ox}^* = −2.10 V vs. SCE). On the other hand, the electron-donating groups, such as *tert*-butyl and amino moieties, significantly enhance the reducing ability of phenothiazine derivatives (**K-T**; E_{ox}^* = −2.13 to −2.90 V vs. SCE). Furthermore, N—H phenothiazine (**Q**) and the benzo[*b*]phenothiazine anion (**U**) exhibit remarkably low excited-state oxidation potentials ($E_o{}^*$ = −2.60 and −3.51 V vs. SCE, respectively). Owing to their broad range of low excited-state oxidation potentials ($E_o{}^*$ = −1.35 to −3.51 V vs. SCE), a variety of

* Corresponding author.
E-mail address: ktanaka@okayama-u.ac.jp (K. Tanaka).

https://doi.org/10.1016/j.tetlet.2025.155745
Received 7 April 2025; Received in revised form 7 July 2025; Accepted 8 July 2025
Available online 11 July 2025

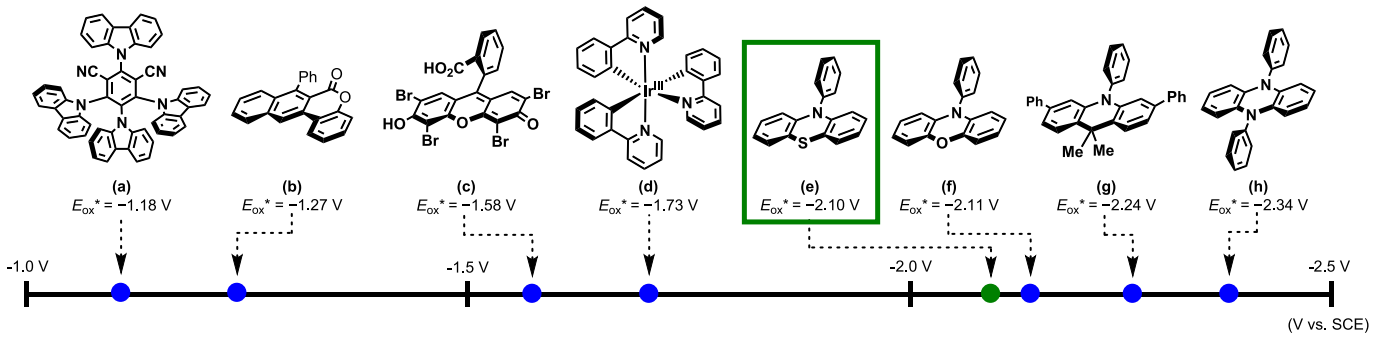

Fig. 1. Representative reducing photoredox catalysts.

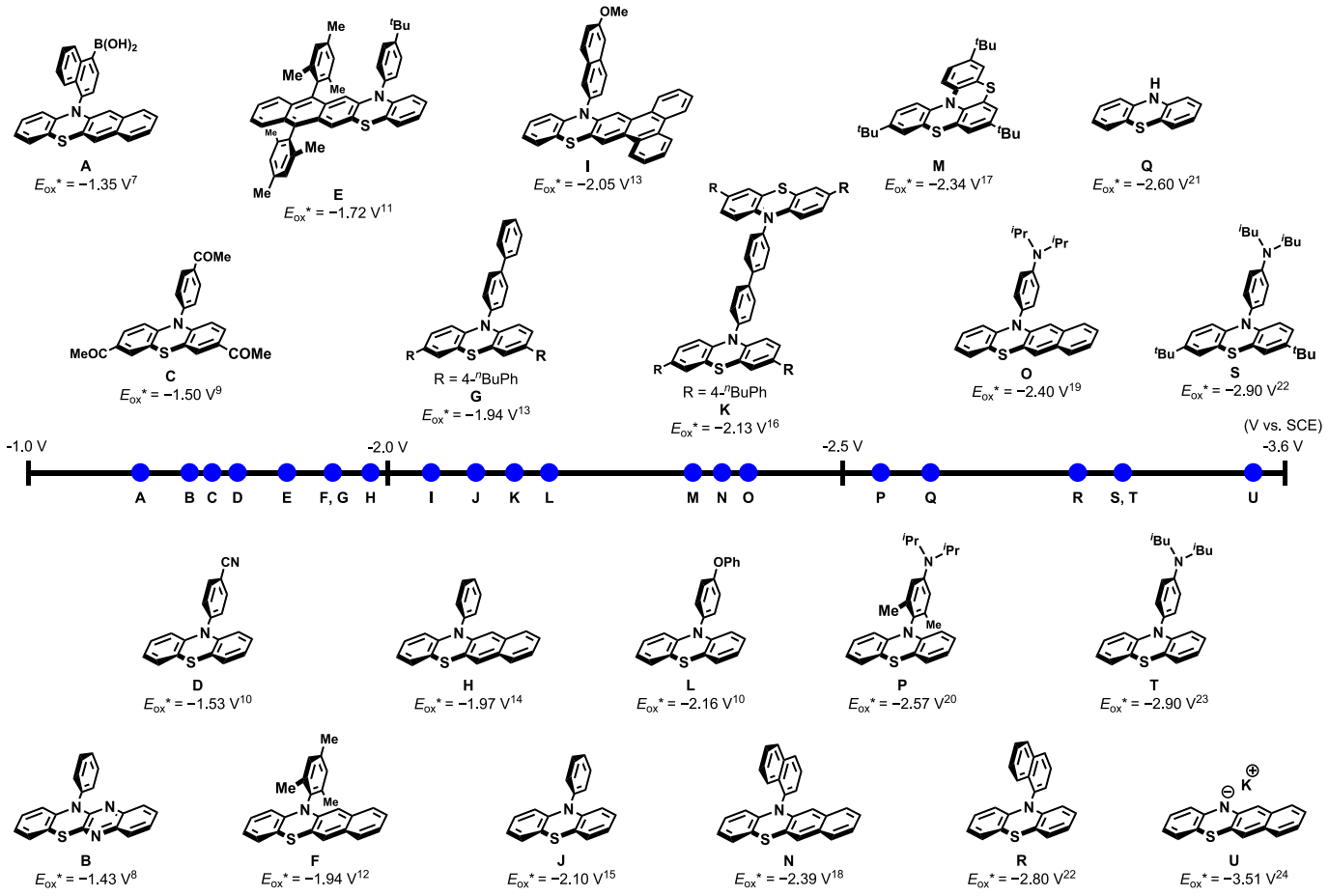

Fig. 2. Chemical structures and E_{ox}^* values of the phenothiazine-based photocatalysts discussed in this review.

photoredox reactions via oxidative-quenching cycles have been successfully developed, including [2+2] cycloadditions, dehalogenative cross-coupling reactions, semipinacol rearrangements, polymerizations, and reactions to generate heterocycles [26–27]. In this type of reaction, as illustrated in Fig. 5, the excitation of the phenothiazine catalyst (Phenothiazine*) via visible-light irradiation enables the one-electron reduction of an electron acceptor (A) to give a radical anion ($A^{\bullet-}$) and the oxidized form of the phenothiazine species (Phenothiazine$^{\bullet+}$). The radical-cation species may then accept an electron from a donor (D) to generate a radical cation ($D^{\bullet+}$) and return the catalyst to the ground-state species (Phenothiazine), thus completing the photocatalytic cycle. Against this background, this review highlights recent advances in phenothiazine organophotoredox catalysis.

*Organophotoredox catalytic systems based on **cat. A***

Takemoto and co-workers have developed a benzophenothiazine/boronic-acid hybrid phenothiazine photocatalyst (Scheme 1; **cat. A**) [7,28]. This hybrid catalyst can activate otherwise redox-inactive carbonyl groups, thus enabling [2 + 2] cycloaddition reactions via a single-electron transfer (SET). While the combination of phenyl boronic acid **3** and an Ir catalyst or **cat. H** did not efficiently produce the cycloadduct (Scheme 1 (a), entries 1–2), **cat. A** increased the product yield substantially (Scheme 1, entry 3). The reaction shown in Scheme 1 afforded various products that include various functional groups, such as a quaternary carbon center (Scheme 1 (b); **2a** and **2b**), a cyclopentyl group (**2c**), a sulfonamide group (**2d**), a phenyl group (**2e**), and a nitrile group (**2f**). The proposed mechanism for the [2 + 2] cycloaddition

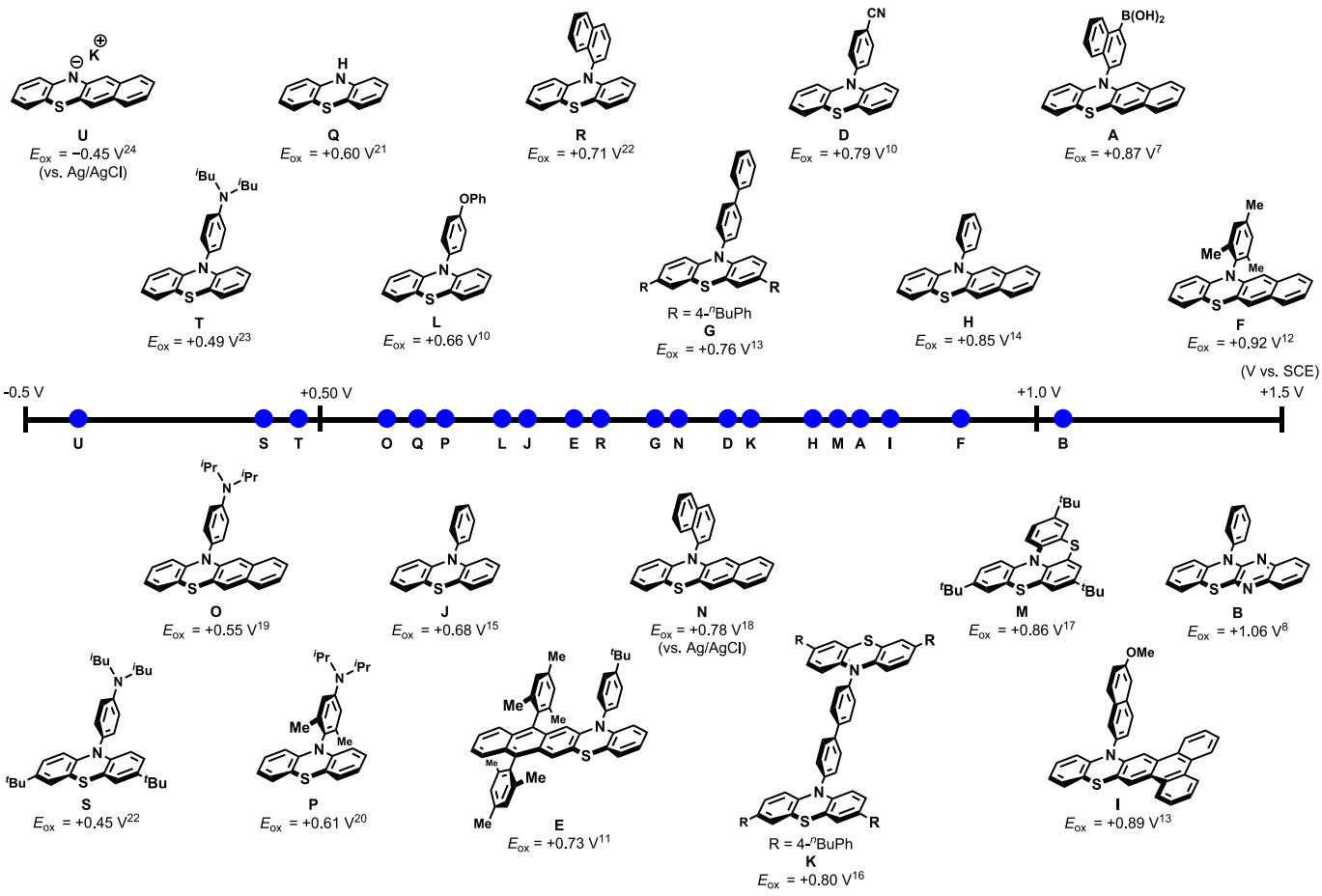

Fig. 3. Chemical structures and E_{ox} values of the phenothiazine-based photocatalysts discussed in this review.

catalyst	A	B	D	E	F	G	H	I	J	K	L	M	N	O	R	S	T
Excitation λ_{max} (nm)	/	412	298	339	362	345	365	353	320	335	318	317	350	/	316	319	317
Emission λ_{max} (nm)	558	497	535	506	435	/	439	/	443	/	440	449	453	375	373	407	449

Fig. 4. UV/Vis absorption and fluorescence maxima of phenothiazine-based photocatalysts.

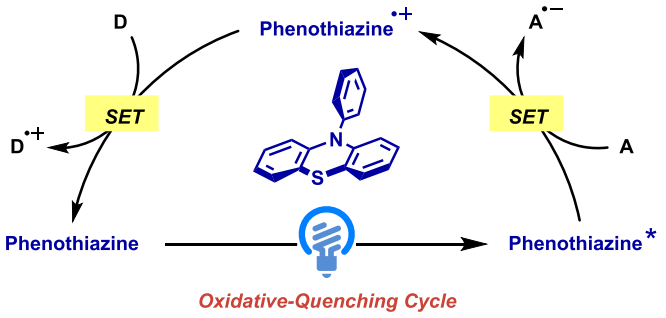

Fig. 5. Phenothiazine organophotoredox catalysis via an oxidative-quenching cycle.

reactions catalyzed by **cat. A** is shown in Scheme 1 (c). First, the carboxylic-acid groups in starting material **1** and the hybrid boronic acid form complex **4** in the presence of MS5A. Subsequently, an SET from the photoexcited hybrid catalyst (**4***) to the complex generates radical anion **5**, from which intermediate **6** can be formed via a five-*exo*-cyclization with the pendant olefin.

Another intramolecular cyclization between the electron-deficient radical and the electron-rich enediolate moiety of **6** affords intermediate **7**, followed by an efficient intramolecular SET to give [2 + 2] cycloadduct **8**. The authors assumed that despite the reversibility of the 4-*exo*-cyclization step, in the case of the dual catalyst system, the ring opening of **7** would occur more efficiently, given the ring strain, than the intermolecular SET from a radical on the carbonyl carbon of **7** to a photocatalyst radical cation. On the other hand, in the hybrid-catalyst system, conversion of **7** to **8** would occur immediately because the final SET step proceeds intramolecularly from the carbonyl-carbon radical to the radical cation of the photocatalyst moiety.

*Organophotoredox catalytic systems based on **cat. B***

Carreira and co-workers have reported the benzothiazinoquinoxaline- (**cat. B**) and cobalt-catalyzed photo-semipinacol rearrangement of unactivated allylic alcohols (Scheme 2) [29]. Both aliphatic and aromatic groups participate as migrating groups in the reaction, yielding a

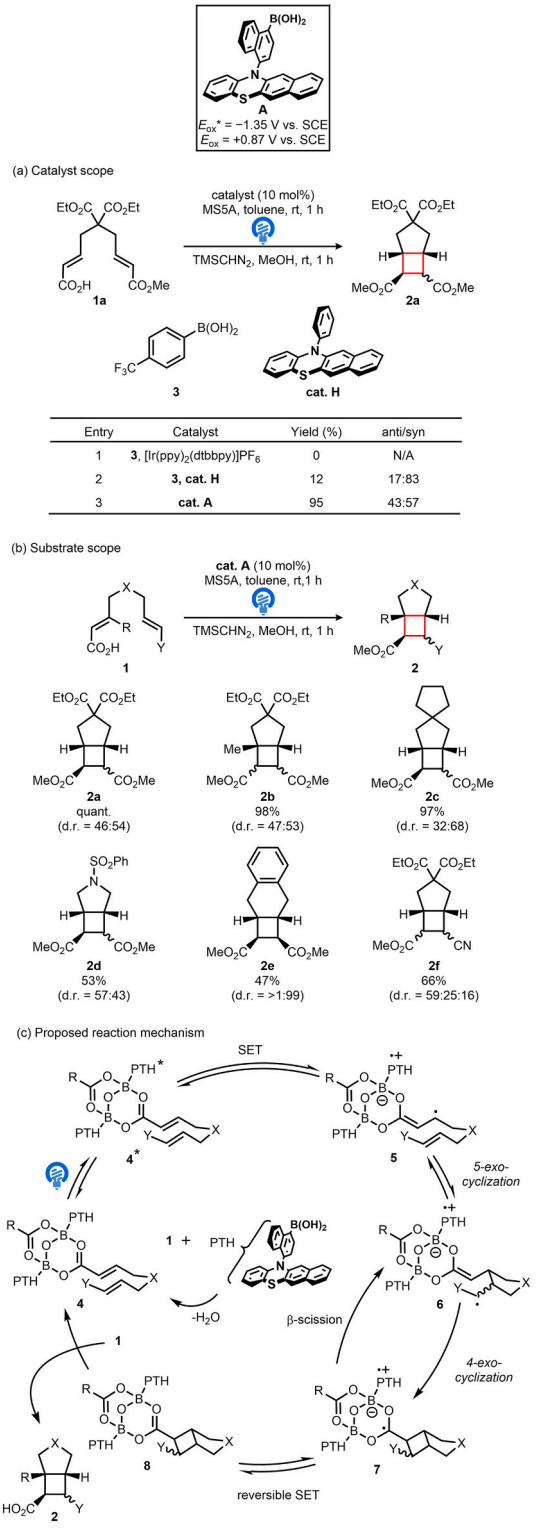

Scheme 1. [2 + 2] Cycloaddition reactions catalyzed by **cat. A**.

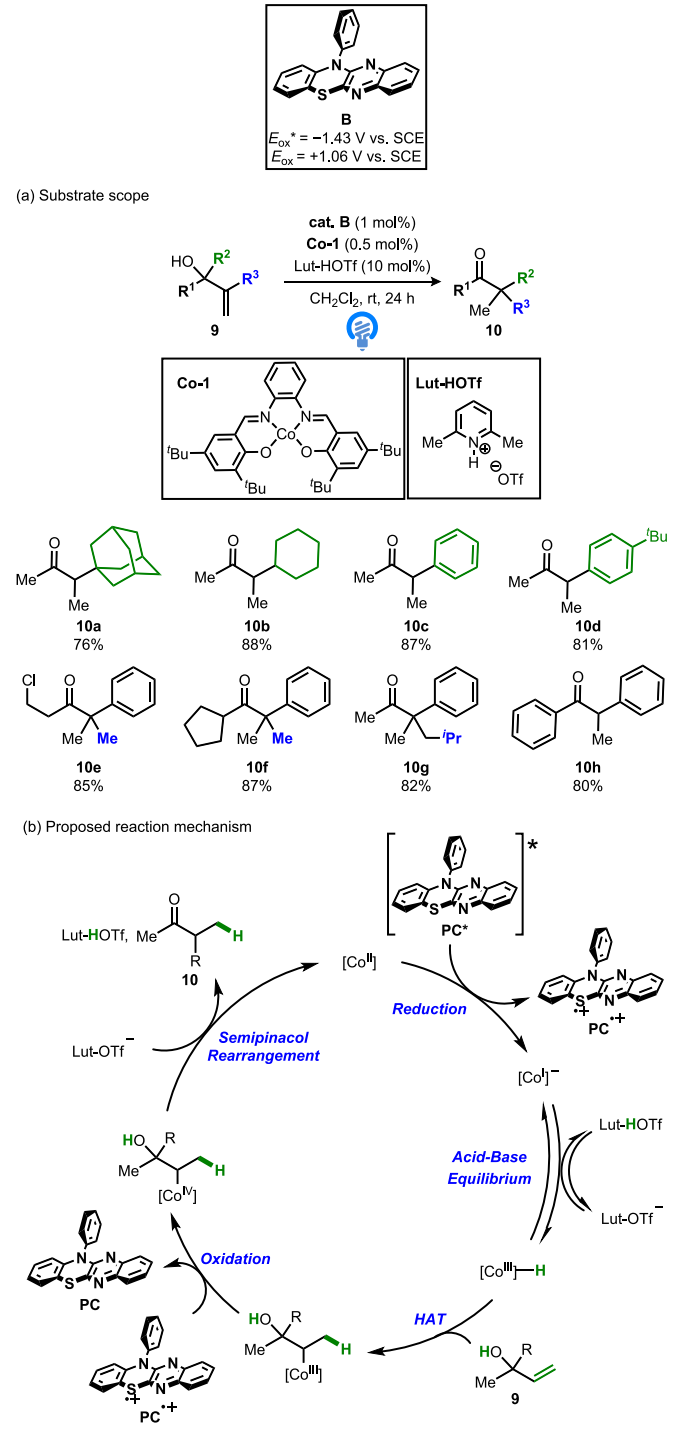

Scheme 2. Photo-induced cobalt-catalyzed semipinacol rearrangement.

variety of α,α-disubstituted ketones (**10a-10d**), whilst a variety of other substituents are also suitable for the reaction (**10e-10h**). A proposed mechanism for the photo-semipinacol reaction is shown in Scheme 2(b). Initially, the [Co^{II}]-salen catalyst (**Co-1**) is reduced by the excited-state photocatalyst (PC*; $E_{ox}^* = -1.43$ V vs. SCE), which results in the formation of an anionic [Co^{I}]$^-$complex, before reversible protonation yields the conjugate acid [Co^{III}]-H. The latter subsequently undergoes addition of an H atom to the unactivated olefin to furnish a more stable secondary [Co^{III}]-alkyl species. This intermediate is oxidized by $PC^{\bullet+}$ to form a [Co^{IV}]-alkyl species that is thought to be in equilibrium with the free carbocation. The base-mediated substitution of the [Co^{IV}]-complex with a concomitant semipinacol rearrangement leads to the formation of the product while the [Co^{II}]-catalyst is regenerated to close the catalytic cycle.

Carreira and co-workers have furthermore expanded the reaction system to enable the synthesis of heterocycles via the cycloisomerization of unactivated olefins (**11**) (Scheme 3). This reaction is amenable to *N*-, *O*-, and *C*-nucleophiles, and yields a number of different heterocycles (**12a-12h**) [30]. The same researchers have also developed two late-stage drug diversification reactions to furnish 2-methylpyrrolidine **12i**

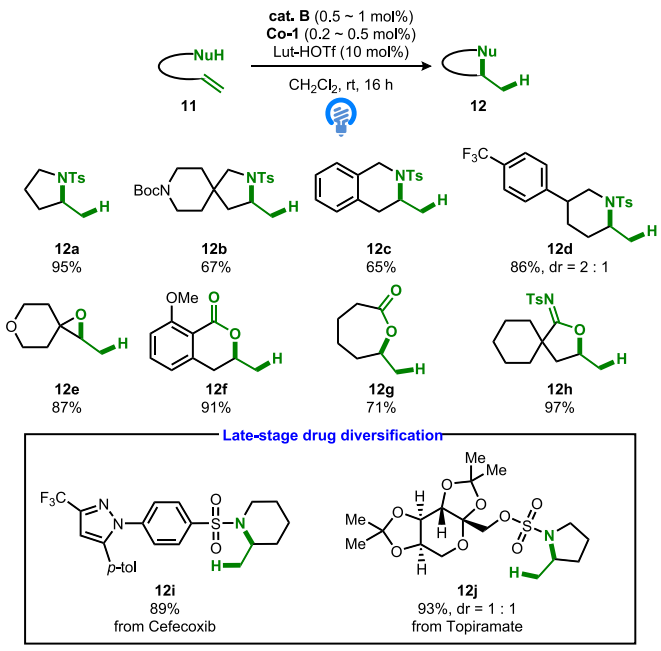

Scheme 3. Photo-induced cobalt-catalyzed synthesis of heterocycles.

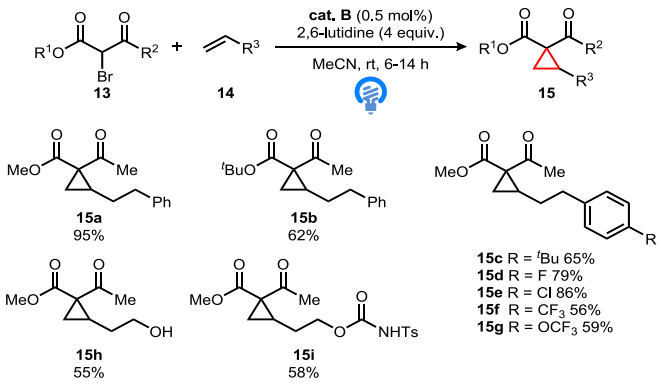

Scheme 4. Intermolecular organophotocatalytic cyclopropanation.

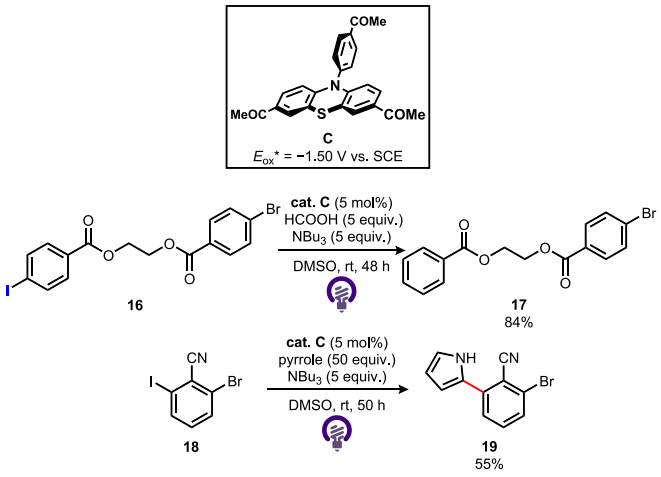

Scheme 5. A chemoselective dehalogenation and a C–C-bond-formation reaction involving aryl halides.

and 2-methylpiperidine **12j** in high yield.

Furthermore, Carreira has reported that **cat. B** can catalyze the intermolecular cyclopropanation of unactivated olefins (Scheme 4) [8]. This transformation shows broad functional-group tolerance and is amenable to both terminal and highly substituted olefins (**15a-15i**).

*Organophotoredox catalytic systems based on **cat. C***

Alaniz, Hawker, and co-workers have developed both a chemoselective dehalogenation and a C–C-bond-formation reaction involving aryl halides (Scheme 5) [9]. **Cat. C** selectively reduces aryl iodide **16** to afford dehalogenated **17** in good yield. Furthermore, the present reaction could also be used to achieve a C − C-bond-formation reaction via a selective dehalogenation to give **19**. Recently, the dehalogenation of aryl halides has been developed via the consecutive photoinduced electron-transfer (ConPET) mechanism using Ph-Acr-Mes and PDI as organophotoredox catalysts [31].

*Organophotoredox catalytic systems based on **cat. D** and **cat. L***

Maity and co-workers have developed a photoredox strategy for installing thiocyanates and isothiocyanates in a controlled chemoselective fashion by manipulating the ambident SCN group through phenothiazine-catalyst modulation (Scheme 6) [10]. The methodology allows redox- and pot-economical on-demand direct access to various hydrothiophenes (**22a-22g**) and pyrrolidine heterocycles (**23a-23g**) from the same feedstock of alkenes and bifunctional thiocyanomalonates via a photocascade sequence.

The mechanism, which allows the formation of these divergent products, is shown in Scheme 6 (b). Initially, an SET from the photoexcited catalyst, **cat D*** (E_{ox}* = −1.53 V vs. SCE) to thiocyanomalonate **21** creates a thiocyanate anion and malonyl radical **24**, which then undergoes addition to alkene **20** to generate radical **25**. This radical proceeds to form **26** via two possible pathways, i.e., a radical-radical cross-coupling or radical-chain transfer. A more plausible route to explain the high efficiency and selectivity observed would be to envision intermediate **25** as a radical-chain mediator that engages with a second molecule of thiocyanomalonate **21**. The metastable species **26** can subsequently undergo Lewis-acid-assisted cyclization to generate *S*-heterocycle **22**. When the more reductively potent **cat. L*** (E_{ox}* = −2.16 V vs. SCE) is used, the previously formed thiocyanate **26** undergoes a second SET that splits it into radical **25** and a thiocyanate anion. From there, if radical **25** is susceptible to being oxidized to a stable carbocation by an oxidative-polar crossover event, the generated carbocation (**27**) can be trapped by the isothiocyanate anion to form thermodynamically stable isothiocyanate **28**, which subsequently cyclizes to afford 2-thiopyrrolidone **23**.

*Organophotoredox catalytic systems based on **cat. E***

Shi and Zhao have reported a novel *N*-aryl-substituted π-extended phenothiazine (**cat. E**) [11]. Extended phenothiazines exhibit a continuous red shift of their absorption when the number of fused rings they incorporate is increased. For example, **cat. E** was used in a visible-light-driven oxidative-coupling reaction of amine **29** to give **30** in excellent yield (Scheme 7).

*Organophotoredox catalytic systems based on **cat. F***

Ohmiya and Nagao have developed a photoredox triple catalyst system that uses **cat. F**, cobalt, and a Brønsted acid for the Markovnikov hydroalkoxylation of unactivated alkenes (Scheme 8) [12]. A variety of alkenes (**32**) were treated with alcohols, water, phenols, and carboxylic acids (**31**) to give the corresponding products (**33a-33j**) in good yield.

The reaction mechanism for this photoredox triple catalyst system is shown in Scheme 8 (b). Under visible-light irradiation, photoredox

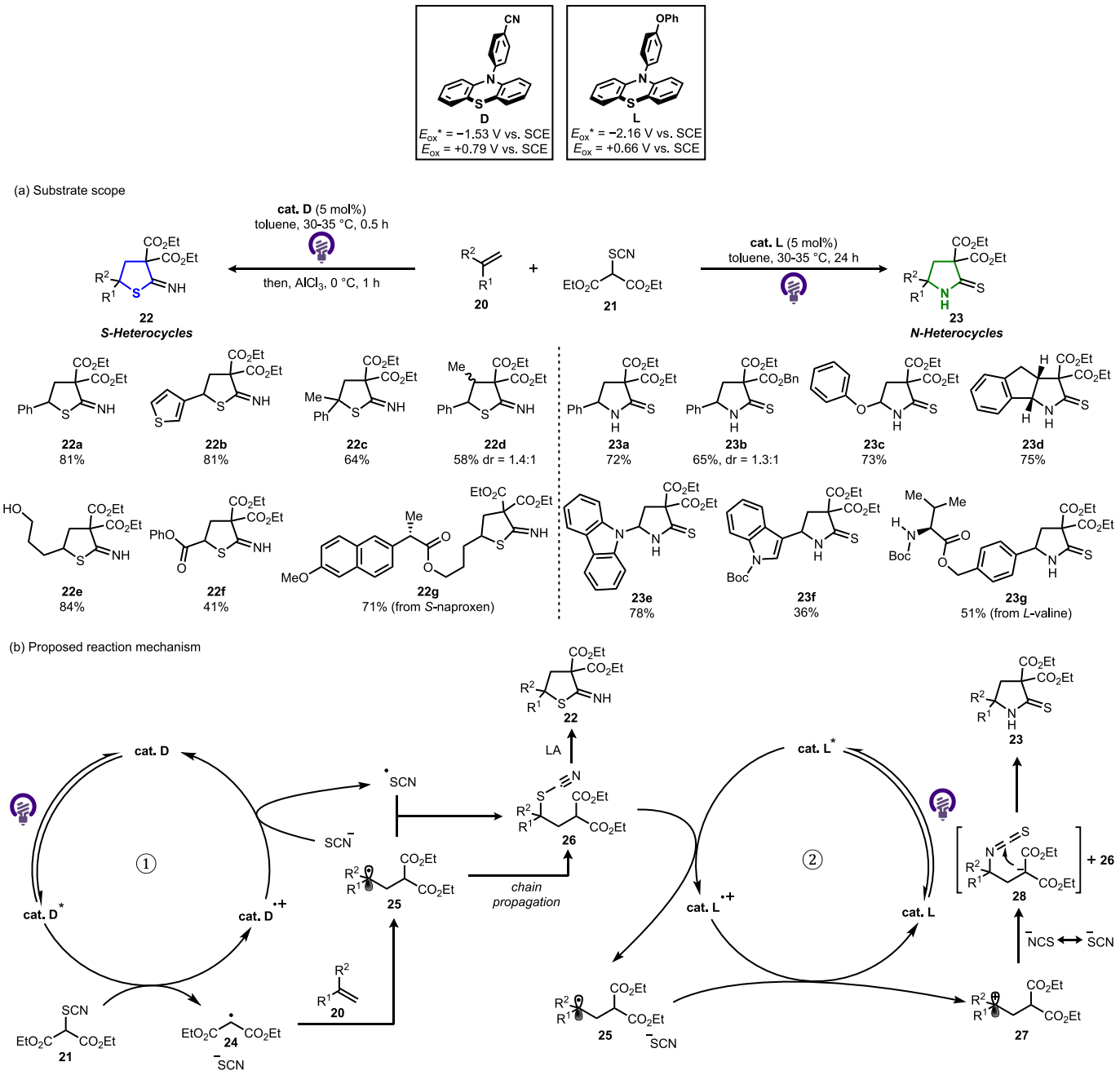

Scheme 6. Chemoselective photocascade of ambident thiocyanates and alkenes via catalyst modulation

catalyst **34** enters excited state **35** with excellent reducing ability (E_{ox}^* = −1.94 V vs. SCE). Subsequently, **35** undergoes an SET with Co(II) (**36**) to form a radical ion pair (**37**). Next, the weak Brønsted acid decomposes **37** into a Co(III) hydride (**38**) and a radical cation of the photoredox catalyst (**39**). The well-known exothermic metal-hydride hydrogen-atom transfer (HAT) from **38** to alkene **32** converts into a Co(II) species (**40**) and an alkyl radical (**41**), which are in equilibrium with an alkyl Co (III) species (**42**). Then, an SET from **39** to **42** generates alkyl Co(IV) species **43** and regenerates **34**. Finally, a substitution reaction between **43** and an alcohol nucleophile (**31**) affords the desired dialkyl ether (**33**) and generates **36** to close the catalytic cycle.

Organophotoredox catalytic systems based on ***cat. G*** *and* ***cat. I***

Chen and co-workers have reported the photo-controlled radical copolymerization of various perfluorinated vinyl-ether monomers and unconjugated comonomers (UCMs) catalyzed by **cat. G** and **cat. I** in the presence of a chain-transfer agent (CTA). The reaction is highly efficient when exposed to visible-light irradiation, affording a large series of main- and sidechain fluorinated copolymers of low dispersity and good chain-end fidelity with excellent conversions of the unconjugated co-monomers (**44**) (Table 1) [13].

Organophotoredox catalytic systems based on ***cat. H***

Ohmiya, Nagao, and co-workers have reported that **cat. H** is able to catalyze a decarboxylative C(sp^3)–O-bond-formation reaction via a radical-polar crossover (RPC; Scheme 9) [14]. Various aliphatic alcohols (**45**) and secondary or tertiary alkyl-carboxylic-acid-derived redox-active esters (**46**) are suitable for this reaction to produce C(sp^3)–O–C (sp^3)-fragment-containing products (**47a-47h**).

Details of the reaction mechanism are shown in Scheme 9 (b). The

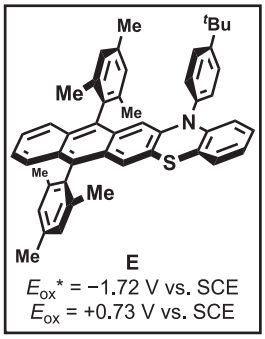

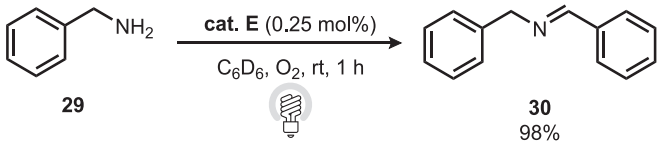

Scheme 7. Photocatalytic oxidative coupling of amine **29**.

catalytic cycle is initiated by the photoexcitation of the phenothiazine catalyst (**cat. H**) using an LED to produce the highly reducing excited state (**cat. H***; $E_{ox}^* = -1.97$ V vs. SCE). Subsequently, **cat. H*** undergoes an SET with redox-active ester **46** to generate the radical cation form of the catalyst (**48**) and alkyl radical **49**. The reaction between **48** and **49** through the SET from **48** to **49** or radical−radical coupling affords alkylsulfonium intermediate **50**. Finally, alcohol nucleophile **45** reacts with the carbocation liberated from **50** to give **47** accompanied by deprotonation and regeneration of the ground state of the phenothiazine catalyst (**cat. H**).

Recently, the authors have extended the semipinacol rearrangement via RPC (Scheme 10) [32]. **Cat. H** facilitates the generation of an α-hydroxy non-benzylic alkyl radical followed by oxidation to the corresponding carbocation, which can be exploited in the semipinacol rearrangement. Thus, the photochemical approach enables a decarboxylative semipinacol rearrangement of β-hydroxycarboxylic acid derivatives (**51**) and an alkylative semipinacol-type rearrangement of allyl alcohols with carbon electrophiles, producing α-quaternary or α-tertiary carbonyls that bear sp^3-rich scaffolds (**52a-52h**).

*Organophotoredox catalytic systems based on **cat. J***

Jui and co-workers have reported the defluoroalkylation of trifluoromethylaromatics (**53**) with unactivated alkenes (**54**) using **cat. J** (Scheme 11) [33,34]. The catalytic system accomplishes the selective cleavage of a single C–F bond in trifluoromethylaromatic substrates (**53**), and the radical intermediates effectively couple with a broad variety of unactivated alkenes (**54**) to afford the corresponding products (**56a-56f**).

A detailed reaction mechanism is shown in Scheme 11 (b). Under irradiation with blue LEDs, excitation of **cat. J** generates the highly reducing excited state, **cat. J*** ($E_{ox}^* = -2.10$ V vs. SCE). An SET to 1,3-bistrifluoromethylbenzene **53a** ($E_{red} = -2.07$ V vs. SCE) delivers the key radical anion (**57**), as well as the oxidized-ground-state catalytic species (**cat. J**$^{\bullet+}$). Radical anion **57** undergoes mesolytic cleavage to eliminate a fluoride ion to deliver electrophilic radical **58**. Intermolecular radical addition to 1-octene **54a** affords nucleophilic radical **59**, which is polarity-matched for a HAT from the electrophilic polarity-reversal catalyst, i.e., cyclohexanethiol (CySH; bond dissociation energy = 86.8 kcal/mol). This step concurrently delivers the desired defluoroalkylation product (**56a**) and the thiyl-radical species. Regeneration of both catalysts by sodium formate closes both catalytic cycles, liberating carbon dioxide and sodium fluoride as the only stoichiometric byproducts.

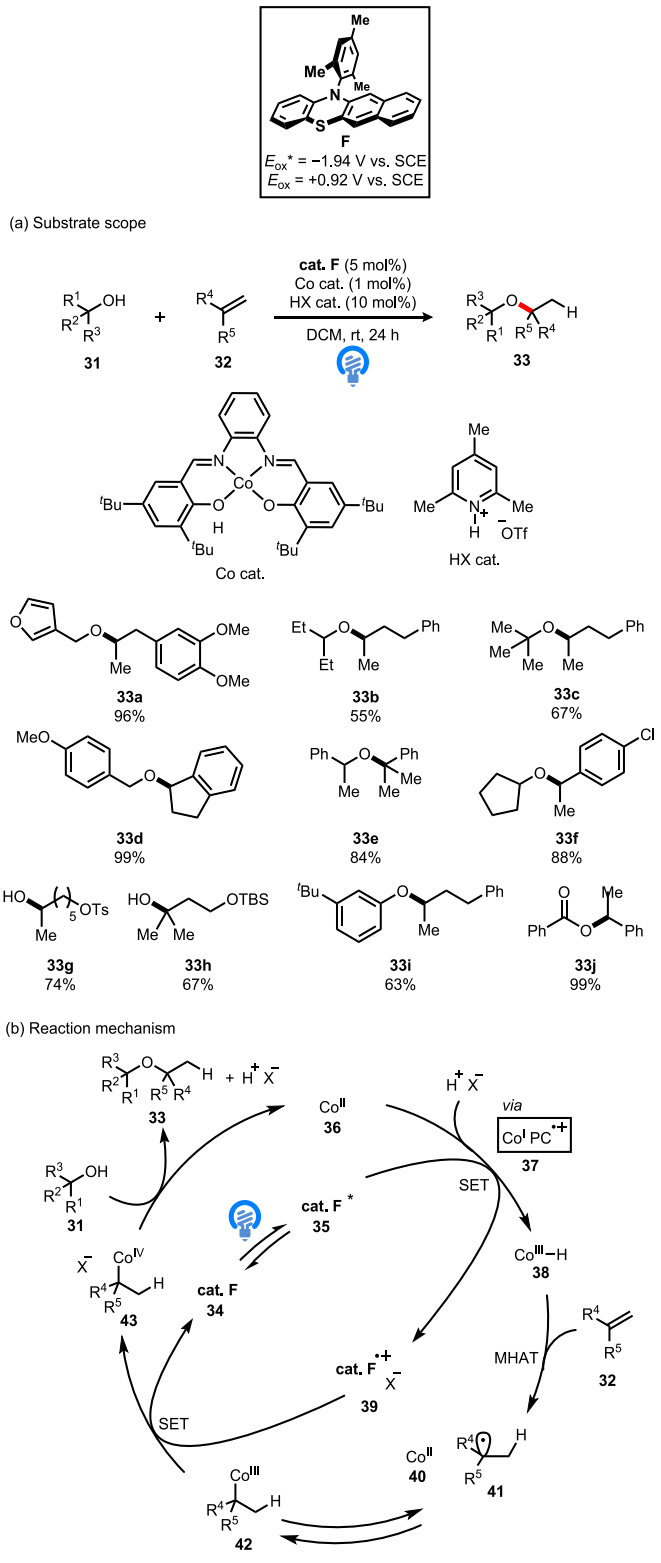

Scheme 8. A photoredox/cobalt/Brønsted-acid triple catalyst system for the Markovnikov hydroalkoxylation of unactivated alkenes.

The reaction system was expanded by Zuo in 2025 to facilitate the cross-coupling of trifluoromethylarene **53a** with heteroarene **60** (Scheme 12) [35]. Furthermore, Xu and co-workers have achieved the construction of a product with a C—S bond (**63**) using **cat. J** [36].

While photocatalytic aryl–aryl cross-coupling reactions have mainly focused on the use of aryl halides or aryl diazonium salts, Procter and co-

Table 1
Controlled organocatalyzed copolymerization of perfluorinated vinyl ethers and unconjugated monomers (UCMs).

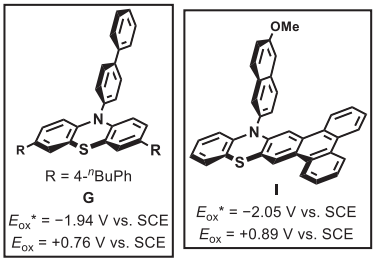

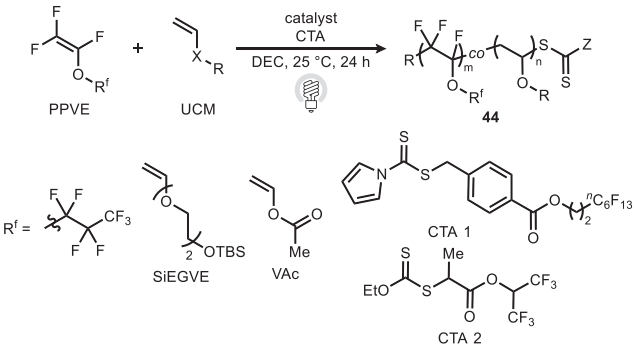

Cat.	UCM	CTA	Conv. (%)	$M_{n,calc}$ [kDa]	$M_{n,SEC}$ [kDa]	$Đ$
Cat. G	SiEGVE	CTA1	>99	26.2	22.0	1.18
Cat. I	VAc	CTA2	>99	13.4	11.2	1.16

worker have developed the C–H/C–H coupling of arenes **64** and **66** catalyzed by **cat. J** (Scheme 13) [37]. The approach is underpinned by the functionalization of a C—H bond in an arene coupling partner using the interrupted Pummerer reaction. The marriage of **cat. J** and the intermediate aryldibenzothiophenium salt **65** is unique and led to a highly selective process that is broad in scope (**67a-67g**).

Xiao, Lan, Lu, and co-workers have developed an asymmetric propargylic radical cyanation enabled by a dual catalyst system consisting of **cat. J** and a copper catalyst (Scheme 14) [38]. Here, **cat. J** generates propargyl radicals and oxidizes the Cu(I) species to a Cu(II) species. A chiral Cu complex functions as an efficient organometallic catalyst to reassemble the propargyl radical and cyanide in an enantio-controlled manner. A diverse range of optically active propargyl cyanides were produced with high reaction efficiency and enantioselectivity (**70a-70g**).

Wickens and co-workers have described a new photocatalytic system that proves that **cat. J** displays latent photooxidant behavior (Scheme 15) [39]. This approach enables oxidative C(sp^2)–N coupling via photooxidation of arene **64** in the presence of $LiClO_4$ and air. This reaction system effectively expands the scope of oxidative photoredox catalysis.

More recently, Glorious, Wenger, and co-workers have reported the synthesis of complex spirocyclic γ-lactones from cyclic malonyl peroxides with olefins activated by phenothiazine sulfoxide (**cat. J-O**: $E_{ox}^* = -1.30$ V vs. SCE, $E_{ox} = +1.35$ V vs. SCE)) generated by **cat. J** (Scheme 16) [40]. Mono- and di-substituted olefines are suitable for this reaction (**75a-75c**). Nonspirocyclic malonyl peroxides can also be successfully transformed into the corresponding lactone (**75d**). Furthermore, products **75e** and **75f**, which bear two spirocenters, and indane were obtained in good yield.

The proposed mechanism is depicted in Scheme 16(b). **Cat. J** is oxidized in situ in the presence of water to give its corresponding sulfoxide (**cat. J-O**). The identified key step for the formation of lactone **75a** is the reductive cleavage of the peroxide bond in **74a** by excited-state

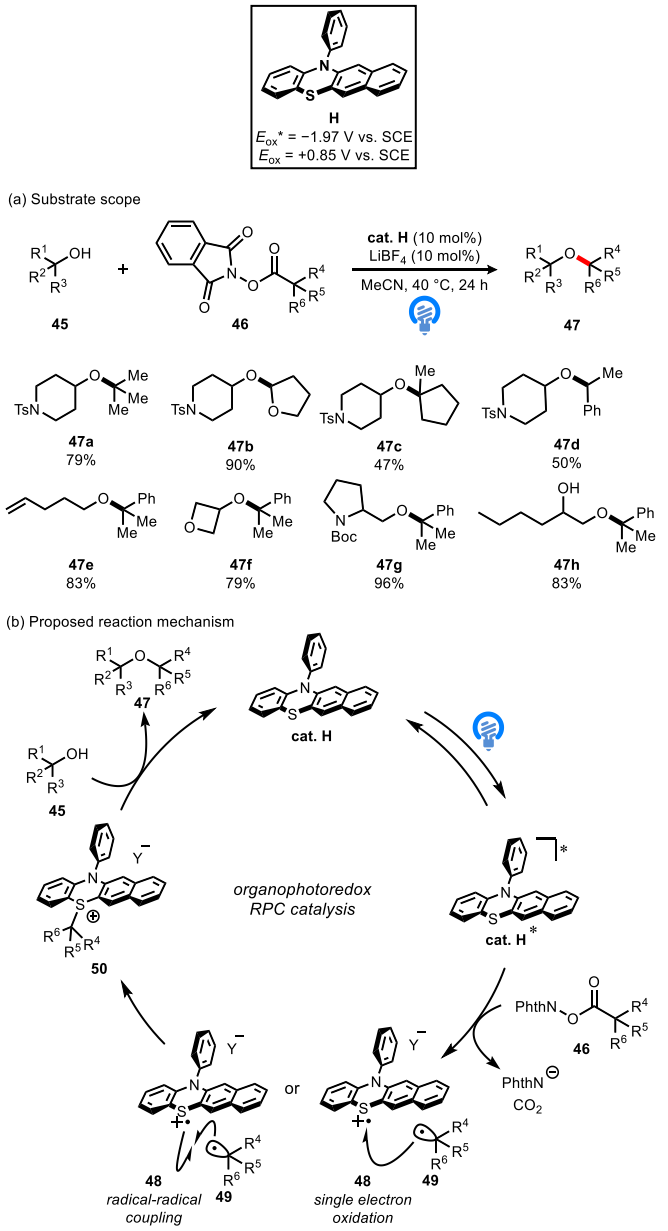

Scheme 9. Decarboxylative C(sp^3) – O bond formation.

cat. J-O*, which is thermodynamically feasible and supported by Stern-Volmer quenching experiments. The resulting radical anion (**76**) rapidly undergoes decarboxylation ($\Delta G = -18.4$ kcal/mol), generating a more stable carbon-centered radical (**77**). This intermediate was confirmed through radical-trapping experiments with both TEMPO and BHT. These radical-trapping studies also support the addition of **77** into styrene **73a**, forming the benzylic radical **78**, which was trapped using BHT. This stabilized radical species ($E_{1/2} = -0.19$ V) can then undergo oxidative radical-polar crossover with the oxidized photocatalyst (**cat. J-O**$^{\bullet+}$) to regenerate the catalyst (**cat. J**) or react with another equivalent of **74a** to initiate a chain-propagation mechanism. Although this latter pathway is thermodynamically feasible and could account for product formation in the dark, the relatively low quantum yield ($\Phi = 0.55$) suggests that the chain propagation is inefficient. Finally, the benzylic cation undergoes intramolecular cyclization with the carboxylate to furnish product **75a**.

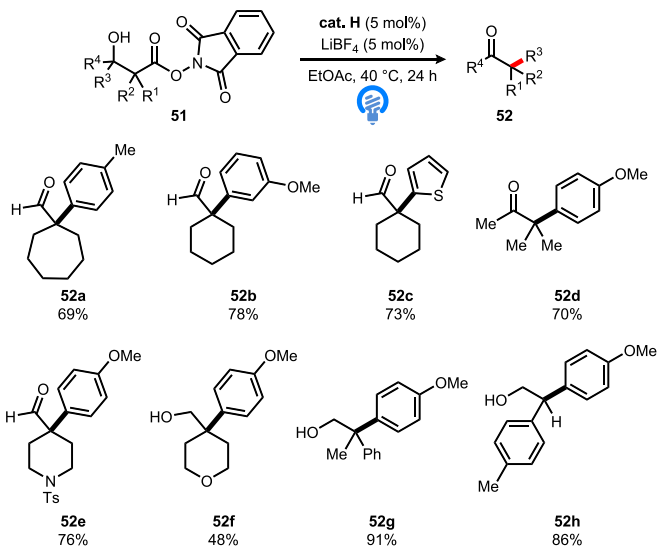

Scheme 10. Semipinacol rearrangement of redox-active esters.

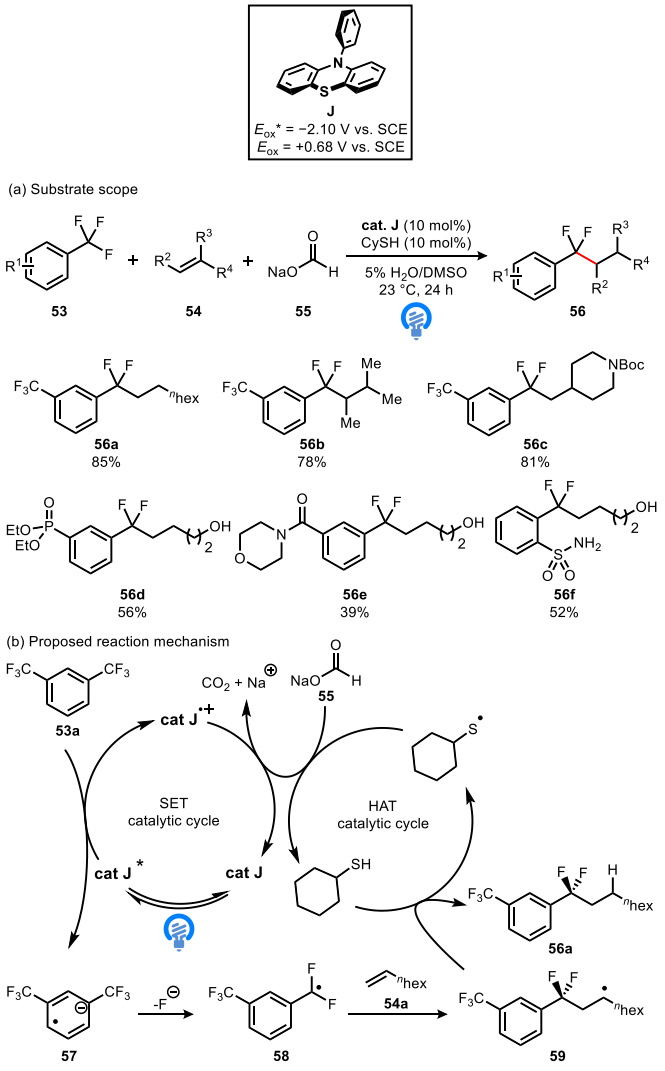

Scheme 11. Catalytic defluoroalkylation of trifluoromethylaromatics with unactivated alkenes.

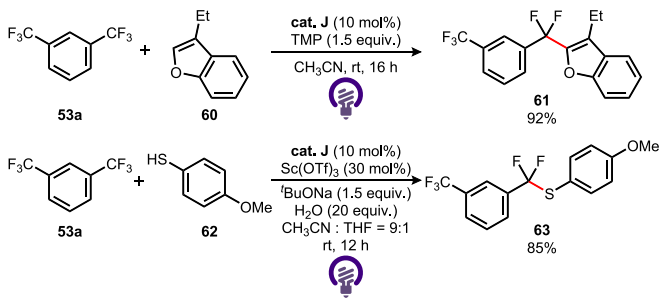

Scheme 12. Functionalization of trifluoromethylarenes using **cat. J**.

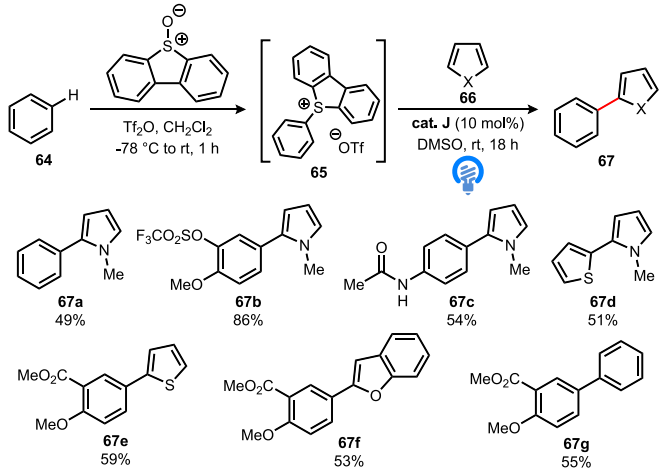

Scheme 13. Formal C–H/C–H coupling of arenes enabled by an interrupted Pummerer reaction.

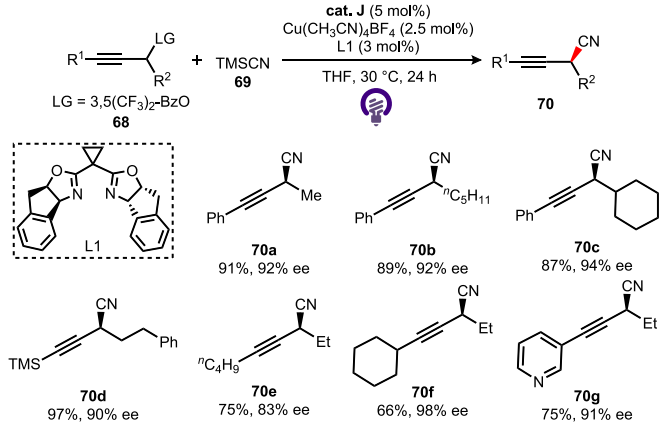

Scheme 14. Asymmetric propargylic radical cyanation mediated using a dual catalyst system.

Scheme 15. Oxidative C—N coupling reaction catalyzed by **cat. J**.

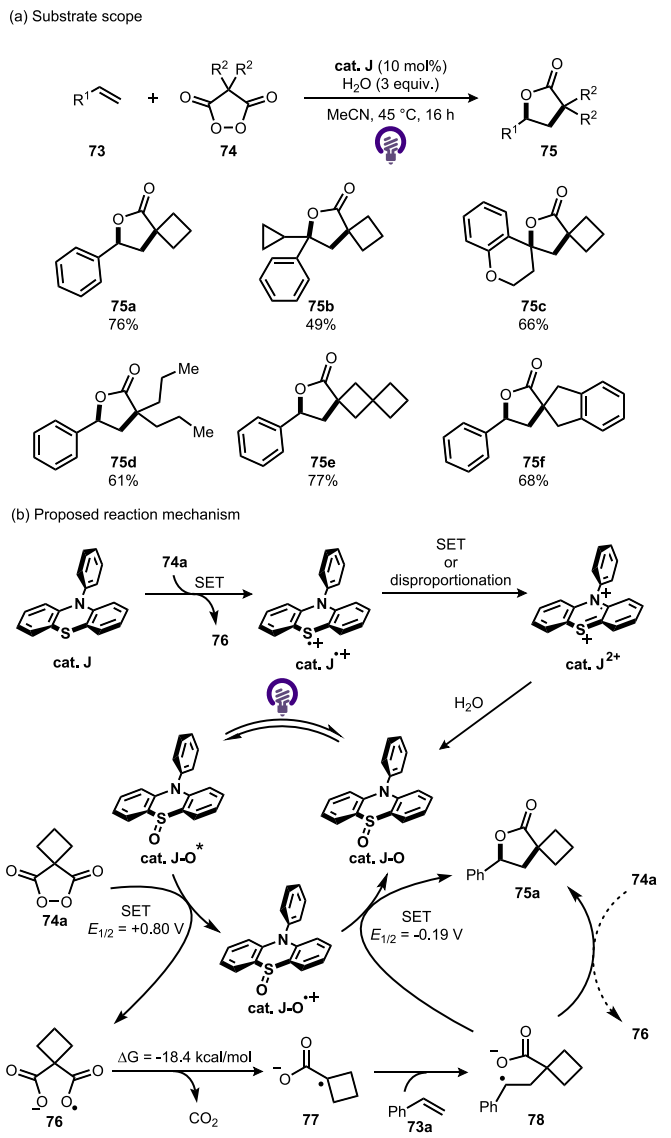

Scheme 16. Phenothiazine sulfoxide as an active photocatalyst for the synthesis of γ-lactones.

*Organophotoredox catalytic systems based on **cat. K***

Chen and *co*-workers have reported a photoredox-mediated reversible-deactivation radical polymerization (RDRPs) via the activation of (hetero)aryl sulfonyl chloride initiators (**79**) with 2,6-lutidine and a newly designed bis(phenothiazine)arene catalyst (**cat. K**; Table 2) [16]. The in-situ-formed sulfonyl pyridinium intermediates effectively promote controlled chain-growth from **79**, thus enabling access to various well-defined polymers (**81**) with high initiation efficiency and controlled dispersity under mild conditions.

*Organophotoredox catalytic systems based on **cat. M***

Our group has developed a strongly reducing and recyclable helical phenothiazine catalyst (**cat. M**) that exhibits a relatively low excited-state oxidation potential (E_{ox}* = −2.34 V vs. SCE; Scheme 17) [17]. **Cat. M** effectively catalyzes the cross-coupling reaction between iodobenzene (**82**) and triethylphosphite to afford aromatic phosphonates in good yield (**83a-83f**). Although **82a** has a low reduction potential (E_{red} = −2.16 V vs. SCE), the SET from **cat. M** to **82a** is energetically favorable due to the low excited-state oxidation potentials of **cat. M**.

Table 2
Initiator-activation strategy to enable an organocatalyzed reversible-deactivation radical polymerization.

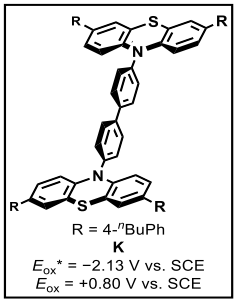

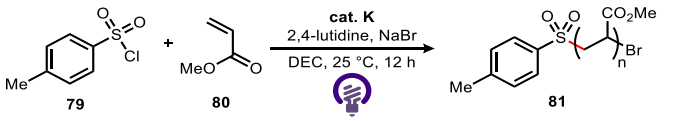

Conv. (%)	$M_{n,calc}$ [kDa]	$M_{n,SEC}$ [kDa]	$Đ$	I*
96	4.4	4.5	1.24	98

When the reaction was performed on the gram scale, the desired product (**83a**) was obtained in 85 % yield (1.20 g) with 96 % recovery of **cat. M** (Scheme 17 (b)). Thus, **cat. M** is a highly active catalyst with high recoverability, even when used on the gram scale. In addition, when **cat. J** was treated with tosyl chloride (TsCl) under blue-LED irradiation, the monosulfonylated product (**84**) was obtained in 78 % yield due to the high reactivity at the *p*-position relative to the nitrogen atom in 10-aryl phenothiazines (Scheme 17 (c)) [25a]. In contrast, **cat. M** was recovered in 95 % yield when subjected to the same conditions, proving that the presence of the ^{t}Bu groups increases the catalyst stability. Therefore, **cat. M** is applicable to various photoredox reactions that cannot be effectively achieved using hitherto reported phenothiazine catalysts.

*Organophotoredox catalytic systems based on **cat. N***

Li and co-workers have reported the difluoroalkylation of unactivated olefins to give difluoromethylene-containing tetrahydropyridazines (Scheme 18) [18]. **Cat. N** effectively catalyzes the radical cascade difluoromethylation/cyclization of *N*-homoallylacetohydrazides (**85**) to give a variety of difluoroalkylated tetrahydropyridazines (**87a-87f**).

*Organophotoredox catalytic systems based on **cat. O**, **cat. R**, and **cat. S***

Wagenknecht and co-workers have also developed various strongly reducing phenothiazine catalysts (**cat. O**, **cat. R**, and **cat. S**; Scheme 19) [19,22]. These catalysts can be used in the nucleophilic addition of methanol to α-methyl styrene (**88**) for the single-electron reduction of **88** (E_{red} ≈ −2.3 to −2.6 V vs. SCE). In the proposed reaction mechanism, after excitation of the catalyst (PC*), an electron is transferred to **88**. The resulting α-methyl styrene radical anion (**90**) is immediately protonated, and the neutral radical (**91**) is formed. A second electron transfer to $PC^{\bullet+}$ converts **91** into the cationic intermediate (**92**), which reacts with methanol to give the final addition product (**89**).

*Organophotoredox catalytic systems based on **cat. P***

Yasuda, Nishimoto, and co-workers have developed a sequential C—F bond transformation of the difluoromethylene unit in a perfluoroalkyl compound (Scheme 20) [20]. **Cat. P** promotes the defluoroaminoxylation of perfluoroalkylarenes **93** with (2,2,6,6-tetramethylpiperidin-1-yl)oxyl (TEMPO, **94**) under visible-light irradiation, affording the corresponding aminoxylated products (**95**).

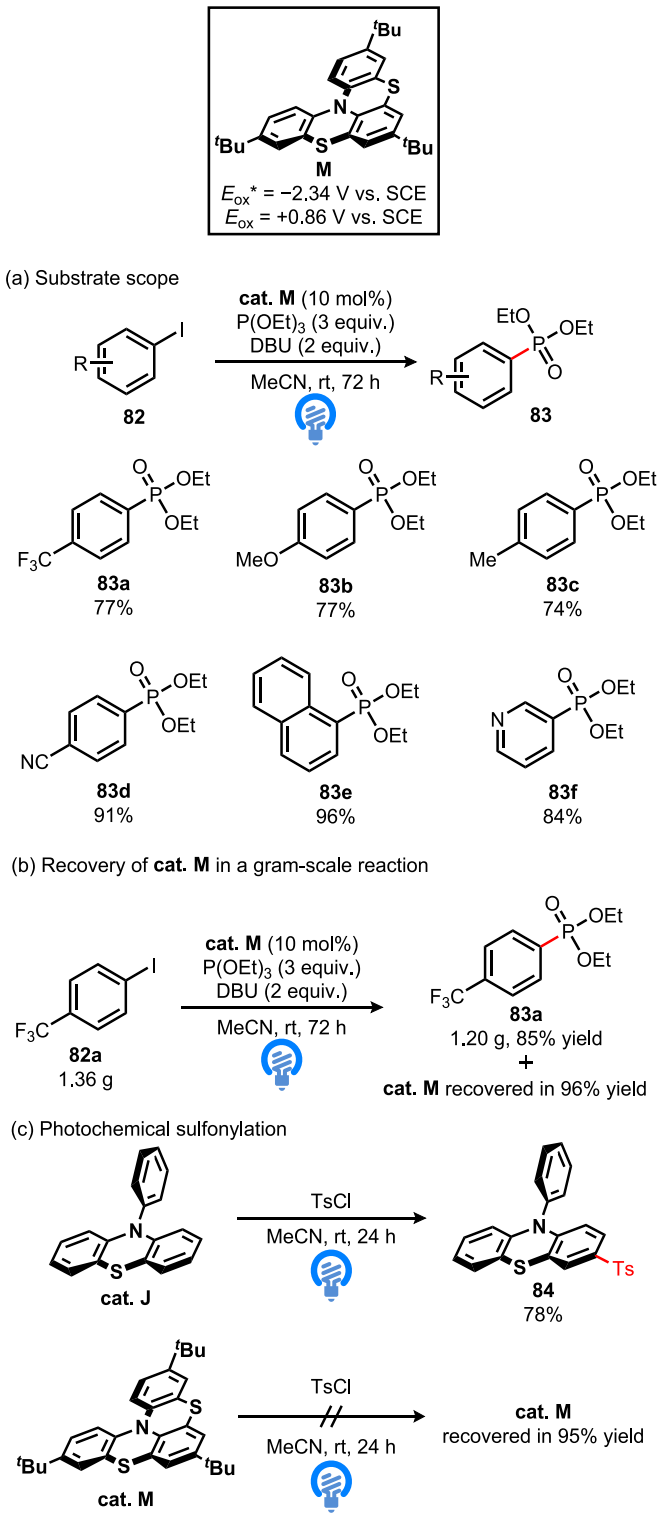

Scheme 17. Phosphonation of aryl iodides with **cat. M**.

Electron-withdrawing and -donating groups on the benzene ring are tolerated during the transformation (**95a-95c**). Substrates including benzofuran and quinoline can be converted efficiently into the corresponding products (**95d** and **95e**). A substrate with two C_4F_9 groups undergoes a single aminoxylation to furnish **95f**.

Scheme 20(b) depicts a plausible mechanism for the aminoxylation of **93** with **94** catalyzed by phenothiazine **cat. P**. The photoexcited **cat. P*** (E_{ox}* = −2.57 V vs. SCE) reduces **93** via an SET, affording radical

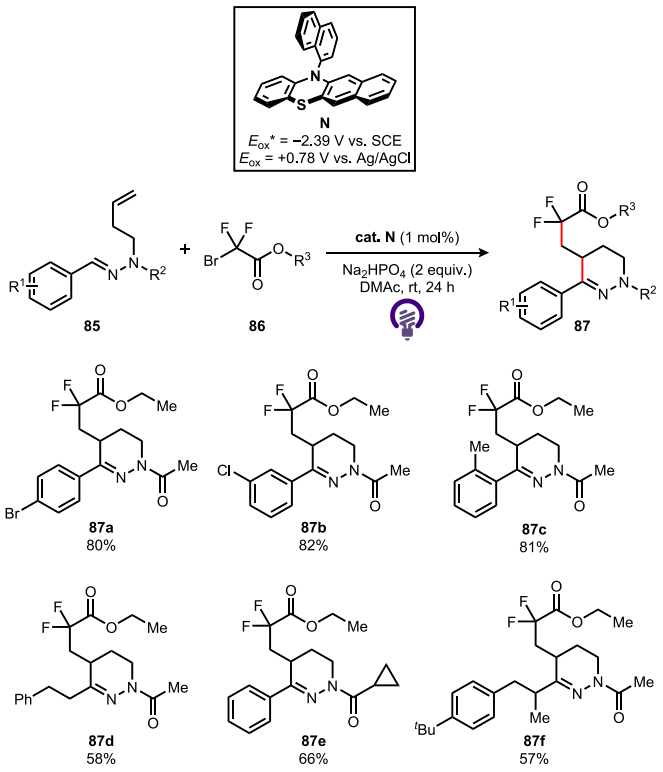

Scheme 18. Difluoroalkylation of unactivated olefins using **cat. N**.

anion **96** and radical cation **cat. P**$^{\bullet+}$. Mesolysis of a C—F bond affords benzyl radical **97**. Then, **97** associates with **94** to give **95**, whilst **cat. P** (E_{ox} = +0.61 V vs. SCE) is regenerated by SET with **94** (E_{ox} = +0.62 V vs. SCE). The cationic *N*-oxoammonium byproduct **98** captures F, suppressing the retro reaction from **97** to **96**. High-resolution mass spectrometry and ^{19}F NMR spectroscopy confirmed that *N*-oxoammonium fluoride **99** is generated. The reduction potential of **cat. P*** is such that it achieves a selective reduction of starting material **93** and not **95**, realizing a single C—F bond transformation without overreduction and side reactions. Aminoxylated **100** undergoes a further defluorinative transformation with allyltrimethylsilane **101** mediated by $AlCl_3$ to provide the highly functionalized perfluoroalkyl alcohol **102**.

*Organophotoredox catalytic systems based on **cat. Q***

Larionov and co-workers have hypothesized that the reductive ability of an appropriately selected organic photocatalyst can be enhanced by proton-coupled electron transfer (PCET), thus enabling photoinduced SET in substrates with very negative reduction potentials (Scheme 21(a)) [21]. In fact, the unsubstituted catalyst **cat. Q** is uniquely active as a photocatalyst for the borylation of aryl phosphate **103a** in the presence of Cs_2CO_3 as a base (Scheme 21(b)). Meanwhile, the mere substitution of the *N*-hydrogen atom of **cat. Q** with a methyl or phenyl group (PTH1 and **cat. J**, respectively) leads to a substantial decrease in catalytic activity. This result is striking, given the comparable excited-state redox properties of the *N*-substituted phenothiazines. The structurally similar PTH2 showed a slightly improved performance, likely due to the stronger reducing character of its more electron-rich core. Notably, none of these photocatalysts has a sufficiently strong reducing singlet-excited state to effect the reduction of electron-rich phosphate **103a** (E_{red} = −2.97 V vs. SCE). A variety of electron-rich and -deficient phosphates are readily borylated (**104b-104i**; Scheme 21(c)).

Laulhé and co-workers have developed a cross-coupling reaction between various aryl halides (**105**) and triethyl phosphite (**106**) to form

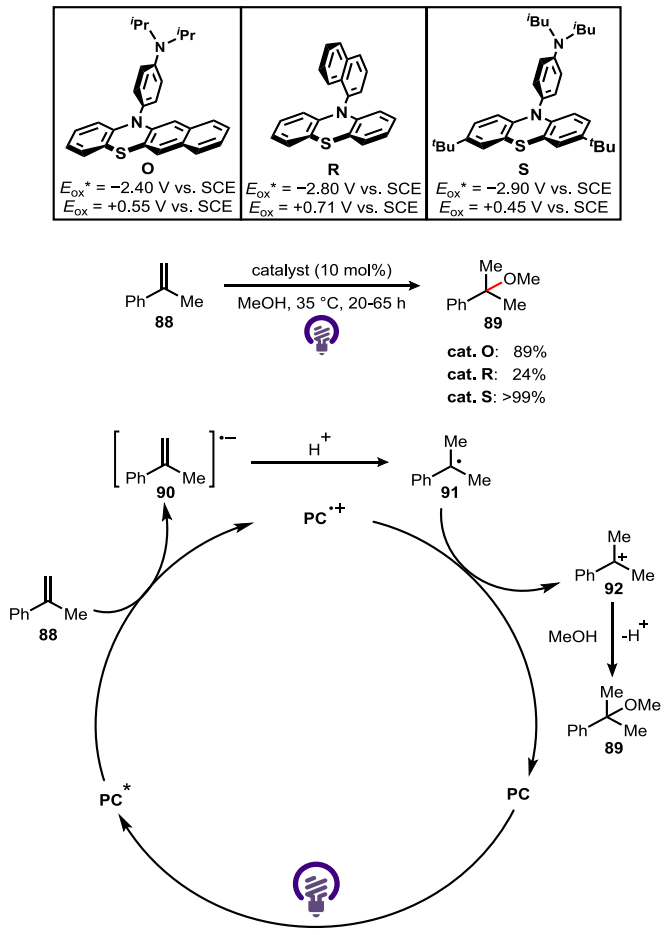

Scheme 19. Photocatalytic reductive activation of α-methyl styrene with **cat. O**, **cat. R**, and **cat. S**.

aromatic phosphonates in an aqueous solvent mixture (Scheme 22) [41]. Various aryl halides are tolerated in this reaction (**107a**-**107g**) and the proposed reaction mechanism is shown in Scheme 22(b). First, photoexcited **cat. Q** reduces aryl halide **105** via an SET to generate aryl radical anion **108**. Loss of a halogen ion produces aryl radical **109**, which then couples with triethyl phosphite (**106**) and forms phosphoranyl radical **110**. Facile oxidation of **110** by **cat Q**$^{\bullet+}$ produces phosphonium species **111** and regenerates the active photocatalyst. Further reaction of phosphonium intermediate **111** with DBU affords the desired final product (**107**). While the reaction proceeds via the direct one-electron reduction of aryl halides, enabled by the strong reducing ability of **cat. Q**, recent studies have demonstrated that C—P and C—B bond formations of aryl halides can also be achieved through the ConPET mechanism [42]. In this context, upon photoexcitation, the photocatalyst undergoes single-electron transfer with a sacrificial electron donor, such as *N,N*-diisopropylethylamine, generating a radical ion pair that includes the photocatalyst radical anion. This radical anion can subsequently absorb a second photon to form an electronically excited radical anion, which possesses a high reduction potential sufficient to activate challenging substrates such as aryl halides. Typical organophotoredox catalysts capable of mediating ConPET reactions include Rhodamine 6G, 4CzIPN, 9,10-dicyanoanthracene, and ^{n}Pr-DMQA^{+} [43].

*Organophotoredox catalytic systems based on **cat. T***

Wagenknecht, Dietzek-Ivanšić, and co-workers have developed a reductive activation of aryl chlorides (Scheme 23) catalyzed by dialkylamino substituted phenothiazine **cat. T** [23]. Aryl chlorides present

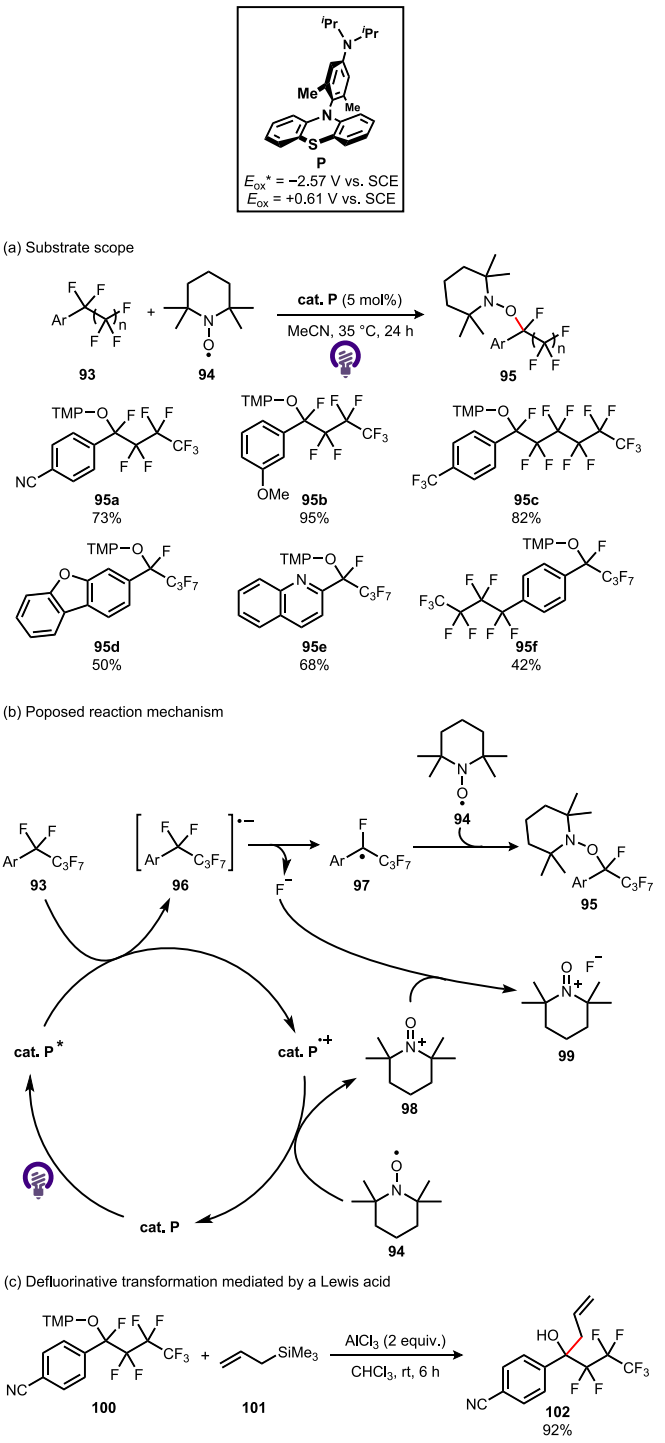

Scheme 20. Sequential C—F bond transformation of the difluoromethylene unit in perfluoroalkyl compounds promoted by **cat. P**.

a particular challenge for photoredox catalytic activation due to the strong C(sp^2)-Cl bond (97 kcal/mol) and its strong reduction potential (E_{red} = −2.80 V vs. SCE). On account of the extremely strong reduction potential of **cat. T** (E_{ox}* = −2.90 V vs. SCE), aryl chlorides with both electron-withdrawing and -donating substituents (**112**) can be activated by photoinduced electron transfer and the corresponding borylation products were obtained (**114a-114h**).

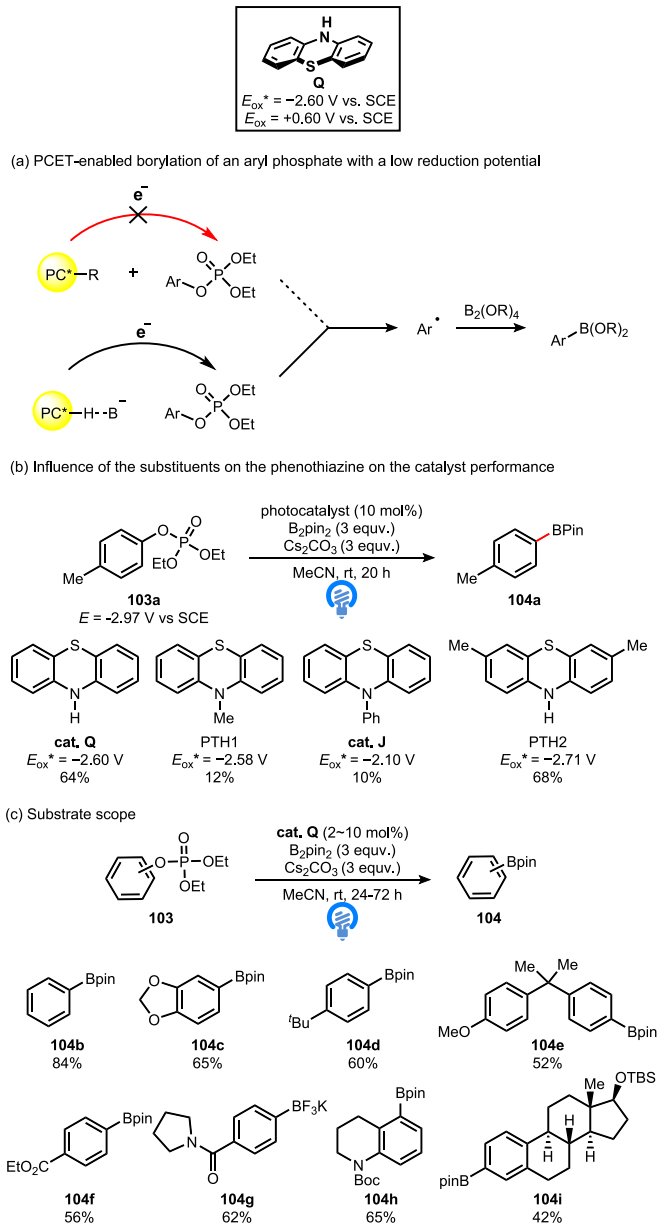

Scheme 21. Borylation of arylphosphates with low reduction potentials.

*Organophotoredox catalytic systems based on **cat. U***

Adhikari and co-workers have discovered that upon excitation by visible light, the benzo[*b*]-phenothiazine anion (**cat. U**) becomes a super-reductant species (Scheme 24) [24]. In contrast to *N*-substituted phenothiazines or benzophenothiazines, **cat. U** exhibits extreme reducing power and can promote SET-based reductive cleavage at a potential of $E_{ox}^* = -3.51$ V vs. SCE. As proof of the utility of **cat. U**, a plethora of aryl-chloride substrates (**115**) were reductively cleaved to fabricate molecules of the isoindolinone class (**116a-116d**). Moreover, aryl-fluoride bonds can be cleaved to generate aryl radicals that were used for C—C-cross-coupling reactions (**118a-118c**). Although the S_NAr reactions of aryl fluorides via a reductive quenching cycle using strongly oxidizing organophotoredox catalysts such as Acr-Mes, TPT, and ^{t}Bu-TTPP have been widely employed [44], one-electron reductive C—F bond transformations have remained largely unexplored. This suggests that the present reaction has significant potential to be developed for broader applications in organophotoredox catalysis involving aryl fluorides.

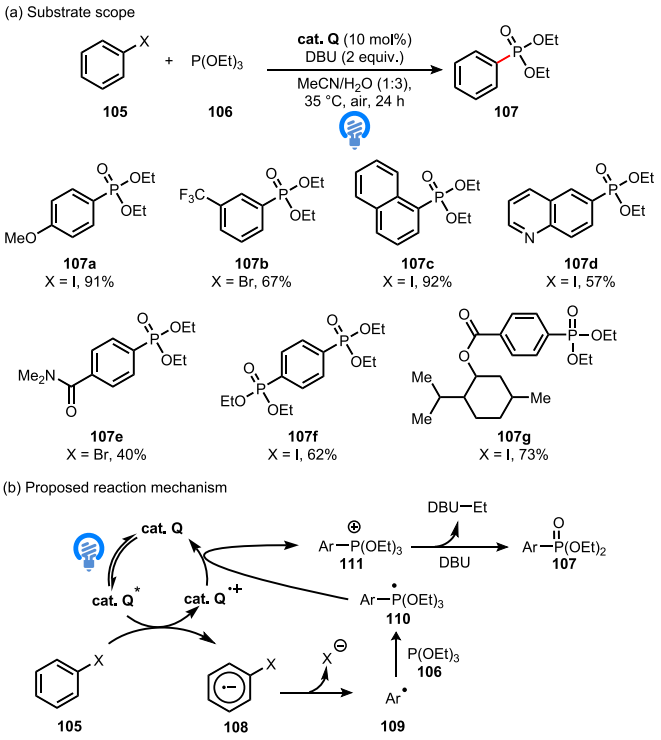

Scheme 22. Phosphonation of aryl halides using **cat. Q**.

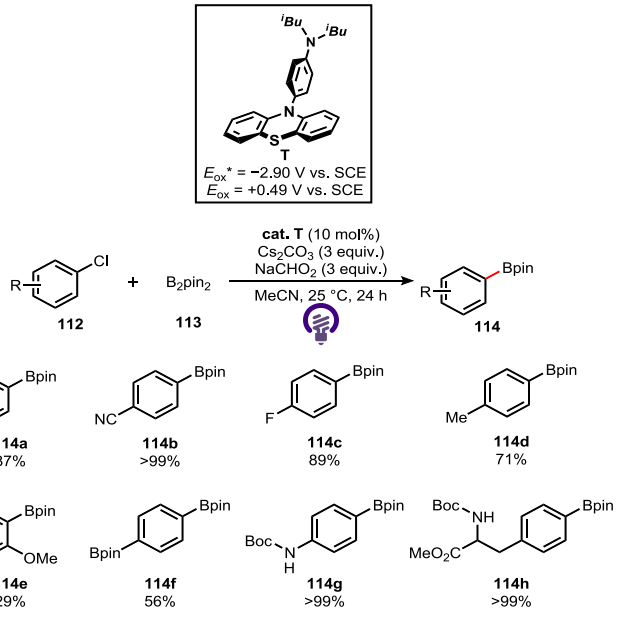

Scheme 23. Borylation of aryl chlorides using **cat. T**.

Conclusions

In recent years, the development of organophotoredox catalysts has advanced significantly, especially with the growing interest in visible-light-driven reactions. Although many highly oxidizing catalysts such as acridinium derivatives are available, there is still a need for efficient catalysts that can act as strong reductants. Phenothiazine-based catalysts, with their low excited-state oxidation potentials, have shown promise as an alternative to expensive iridium-based photocatalysts and, in some cases, have even outperformed them. These catalysts have been successfully applied to a variety of organic reactions, including

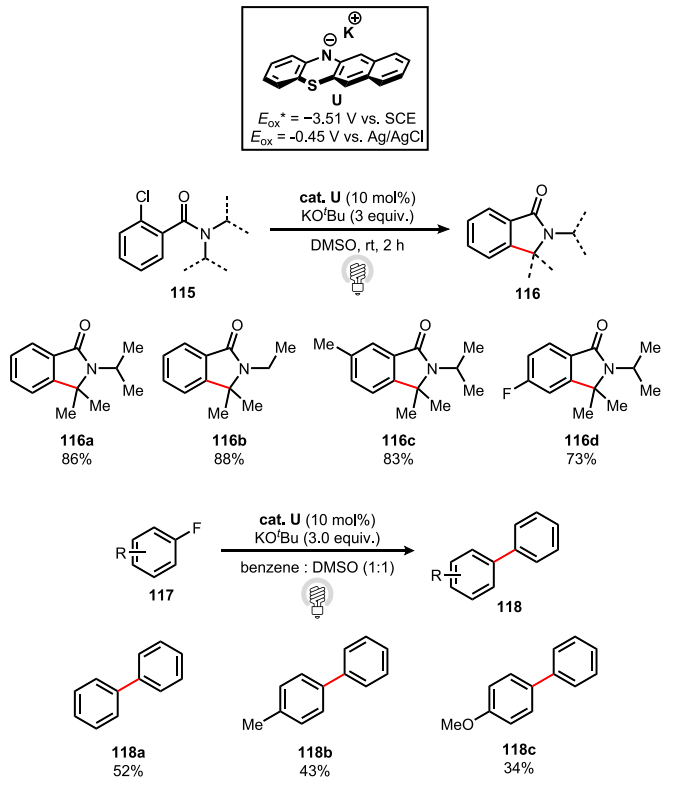

Scheme 24. C—Cl and C—F bond formation catalyzed by **cat. U**.

cycloadditions, cross-coupling, rearrangements, polymerizations, and heterocycle synthesis. However, the use of phenothiazine catalysts in natural product synthesis, biological applications, and materials science is still limited. Further research in these areas may open new possibilities and wider applications for this class of catalysts. It is hoped that this review will inspire future studies and contribute to the growth of organophotoredox catalysis.

CRediT authorship contribution statement

Kenta Tanaka: Writing – review & editing, Writing – original draft. **Hiroyoshi Takamura:** Writing – review & editing. **Isao Kadota:** Writing – review & editing.

Declaration of competing interest

The authors declare that they have no known competing financial interests or personal relationships that could have appeared to influence the work reported in this paper.

Acknowledgements

This work was supported by Wesco Scientific Promotion Foundation, and Electric Technology Research Foundation of Chugoku.

Data availability

Data will be made available on request.

References

[1] (a) C.K. Prier, D.A. Rankic, D.W.C. MacMillan, Visible light photoredox catalysis with transition metal complexes: applications in organic synthesis, Chem. Rev. 113 (2013) 5322–5363;
(b) N. Holmberg-Douglas, D.A. Nicewicz, Photoredox-catalyzed C–H functionalization reactions, Chem. Rev. 122 (2022) 1925–2016;
(c) N.A. Romero, D.A. Nicewicz, Organic photoredox catalysis, Chem. Rev. 116 (2016) 10075–10166;
(d) S. Wu, J. Kaur, T.A. Karl, X. Tian, J.P. Barham, Synthetic molecular photoelectrochemistry: new frontiers in synthetic applications, mechanistic insights and scalability, Angew. Chem. Int. Ed. 61 (2022) e202107811;
(e) Y. Wu, D. Kim, T.S. Teets, Photophysical properties and redox potentials of photosensitizers for organic photoredox transformations, Synlett 33 (2022) 1154–1179.

[2] (a) S. Roy, T. Besset, New opportunities to access fluorinated molecules using organophotoredox catalysis via C(sp3)–F bond cleavage, JACS Au 5 (2025) 466–485;
(b) A. Vega Peñaloza, J. Mateos, X. Companyó, M. Escudero Casao, L. Dell'Amico, A rational approach to organo-photocatalysis: novel designs and structure-property relationships, Angew. Chem. Int. Ed. 60 (2021) 1082–1097;
(c) T. Bortolato, S. Cuadros, G. Simionato, L. Dell'Amico, The advent and development of organophotoredox catalysis, Chem. Commun. 58 (2022) 1263–1283;
(d) N. Noto, S. Saito, Arylamines as more strongly reducing organic photoredox catalysts than *fac*-[Ir(ppy)3], ACS Catal. 12 (2022) 15400–15415;
(e) Y. Lee, M.S. Kwon, Emerging organic photoredox catalysts for organic transformations, Eur. J. Org. Chem. 2020 (2020) 6028–6043;
(f) M.V. Bobo, J.J. Kuchta, A.K. Vannucci, Recent advancements in the development of molecular organic photocatalysts, Org. Biomol. Chem. 19 (2021) 4816–4834.

[3] Naphthochromenone: J. Mateos, F. Rigodanza, A. Vega-Peñaloza, A. Sartorel, M. Natali, T. Bortolato, G. Pelosi, X. Companyó, M. Bonchio, L. Dell'Amico, Naphthochromenones: organic bimodal photocatalysts engaging in both oxidative and reductive quenching processes Angew. Chem. Int. Ed. 59 (2020) 1302–1312.

[4] (a) Phenoxazine: B.G. McCarthy, R.M. Pearson, C.-H. Lim, S.M. Sartor, N. H. Damrauer, G.M. Miyake, Structure–property relationships for tailoring phenoxazines as reducing photoredox catalysts J. Am. Chem. Soc. 140 (2018) 5088–5510;
(b) R.M. Pearson, C.-H. Lim, B.G. McCarthy, C.B. Musgrave, G.M. Miyake, Organocatalyzed atom transfer radical polymerization using N-Aryl phenoxazines as photoredox catalysts, J. Am. Chem. Soc. 138 (2016) 11399–11407;
(c) Y. Fan, Z. Huang, Y. Lu, S. Zhu, L. Chu, Defluorinative alkylboration of alkenes enabled by dual photoredox and copper catalysis, Angew. Chem. Int. Ed. 63 (2024) e202315974;
(d) D.A. Corbin, C. Cremer, K.O. Puffer, B.S. Newell, F.W. Patureau, G.M. Miyake, Effects of the chalcogenide identity in *N*-aryl phenochalcogenazine photoredox catalysts, ChemCatChem 14 (2022) e202200485.

[5] (a) Dihydrophenazine: S.-Y. Li, X.-Y. Yang, P.-H. Shen, L. Xu, J. Xu, Q. Zhang, H.-J. Xu, Selective defluoroalkylation and hydrodefluorination of trifluoromethyl groups photocatalyzed by dihydroacridine derivatives J. Organomet. Chem. 88 (2023) 17284–17296;
(b) B.L. Buss, C. Lim, G.M. Miyake, Dimethyl dihydroacridines as photocatalysts in organocatalyzed atom transfer radical polymerization of acrylate monomers, Angew. Chem. Int. Ed. 59 (2020) 3209–3217;
(c) T. Bortolato, G. Simionato, M. Vayer, C. Rosso, L. Paoloni, E.M. Benetti, A. Sartorel, D. Lebœuf, L. Dell'Amico, The rational design of reducing organophotoredox catalysts unlocks proton-coupled electron-transfer and atom transfer radical polymerization mechanisms, J. Am. Chem. Soc. 145 (2023) 1835–1846;
(d) A.K. Jaiswal, B.B. Skjelstad, S. Maeda, D.C.-Y. Huang, Mechanistic exploration of N-heterocyclic carbene boranes as the hydrogen atom transfer reagent in selective hydrodefluorination reactions, *ACS Catal.* 14 (2024) 17547–17555;
(e) Y. Liu, Q. Chen, Y. Tong, Y. Ma, 9,9-Dimethyl dihydroacridine-based organic photocatalyst for atom transfer radical polymerization from modifying "unstable" electron donor, Macromolecules 53 (2020) 7053–7062;
(f) Y. Zou, S. Li, R. Wang, L. Xu, X. Xu, H. Xu, J. Xu, An NADH model (10-benzyl-9,10-dihydroacridine) enabled radical borylation of C(sp2)–X bonds, Tetrahedron Lett. 143 (2024) 155116.

[6] (a) Dihydrophenazine: J.C. Theriot, C.-H. Lim, H. Yang, M.D. Ryan, C. B. Musgrave, G.M. Miyake, Organocatalyzed atom transfer radical polymerization driven by visible light Science 352 (2016) 1082–1086;
(b) K.O. Puffer, B.S. Portela, A.J. Olson-Gwin, K.A. Chism, S. Dworakowska, E. J. Crace, R.S. Paton, G.M. Miyake, Influence of dihydrophenazine photoredox catalyst excited state character and reduction potentials on control in organocatalyzed atom transfer radical polymerization, ACS Catal. 15 (2025) 5002–5013;
(c) K.O. Puffer, D.A. Corbin, G.M. Miyake, Impact of alkyl core substitution kinetics in diaryl dihydrophenazine photoredox catalysts on properties and performance in O-ATRP, ACS Catal. 13 (2023) 14042–14051;
(d) A. Tlahuext-Aca, L. Candish, R.A. Garza-Sanchez, F. Glorius, Decarboxylative olefination of activated aliphatic acids enabled by dual organophotoredox/copper catalysis, ACS Catal. 8 (2018) 1715–1719;
(e) J.P. Cole, C.R. Federico, C.-H. Lim, G.M. Miyake, Photoinduced organocatalyzed atom transfer radical polymerization using low ppm catalyst loading, Macromolecules 52 (2019) 747–754;
(f) M.D. Ryan, J.C. Theriot, C. Lim, H.G. Yang, A. Lockwood, N.G. Garrison, S. R. Lincoln, C.B. Musgrave, G.M. Miyake, Solvent effects on the intramolecular charge transfer character of N,N-diaryl dihydrophenazine catalysts for organocatalyzed atom transfer radical polymerization, J. Polym. Sci. Part A: Polym. Chem. 55 (2017) 3017–3020.

[7] T. Yumura, T. Nanjo, Y. Takemoto, A benzophenothiazine/boronic acid hybrid photocatalyst enables the single electron transfer (SET) to carboxy groups: SET-

initiated cyclization of α,β-unsaturated carboxylic acids, ACS Catal. 13 (2023) 12803–12809.
[8] D.M. Fischer, H. Lindner, W.M. Amberg, E.M. Carreira, Intermolecular organophotocatalytic cyclopropanation of unactivated olefins, J. Am. Chem. Soc. 145 (2023) 774–780.
[9] S.O. Poelma, G.L. Burnett, E.H. Discekici, K.M. Mattson, N.J. Treat, Y. Luo, Z. M. Hudson, S.L. Shankel, P.G. Clark, J.W. Kramer, C.J. Hawker, J. Read De Alaniz, Chemoselective radical dehalogenation and C–C bond formation on aryl halide substrates using organic photoredox catalysts, J. Organomet. Chem. 81 (2016) 7155–7160.
[10] I.U. Hoque, A. Samanta, S. Pramanik, S.R. Chowdhury, R. Lo, S. Maity, Photocascade chemoselective controlling of ambident thio(seleno)cyanates with alkenes via catalyst modulation, Nat. Commun. 15 (2024) 5739.
[11] J. Zhou, L. Mao, M.-X. Wu, Z. Peng, Y. Yang, M. Zhou, X.-L. Zhao, X. Shi, H.-B. Yang, Extended phenothiazines: synthesis, photophysical and redox properties, and efficient photocatalytic oxidative coupling of amines, Chem. Sci. 13 (2022) 5252–5260.
[12] M. Nakagawa, Y. Matsuki, K. Nagao, H. Ohmiya, A triple photoredox/cobalt/Brønsted acid catalysis enabling markovnikov hydroalkoxylation of unactivated alkenes, J. Am. Chem. Soc. 144 (2022) 7953–7959.
[13] Q. Quan, Y. Zhao, K. Chen, H. Zhou, C. Zhou, M. Chen, Organocatalyzed controlled copolymerization of perfluorinated vinyl ethers and unconjugated monomers driven by light, ACS Catal. 12 (2022) 7269–7277.
[14] (a) S. Shibutani, T. Kodo, M. Takeda, K. Nagao, N. Tokunaga, Y. Sasaki, H. Ohmiya, Organophotoredox-catalyzed decarboxylative C(sp3)–O bond formation, J. Am. Chem. Soc. 142 (2020) 1211–1216;
(b) R. Kobayashi, S. Shibutani, K. Nagao, Z. Ikeda, J. Wang, I. Ibáñez, M. Reynolds, Y. Sasaki, H. Ohmiya, Decarboxylative N-alkylation of azoles through visible-light- mediated organophotoredox catalysis, Org. Lett. 23 (2021) 5415–5419;
(c) Y. Takekawa, T. Kodo, K. Nagao, H. Kakei, K. Takeuchi, Y. Sasaki, H. Ohmiya, Light-driven radical-polar crossover catalysis enabling decarboxylative fluorination of redox active esters, Chem. Lett. 52 (2023) 41–43;
(d) T. Matsuo, K. Nagao, H. Ohmiya, Light-driven radical-polar crossover catalysis for cross-coupling with organosilanes, Tetrahedron Lett. 112 (2022) 154231;
(e) S. Shibutani, K. Nagao, H. Ohmiya, Organophotoredox-catalyzed three-component coupling of heteroatom nucleophiles, alkenes, and aliphatic redox active esters, Org. Lett. 23 (2021) 1798–1803;
(f) M. Nakagawa, K. Nagao, Z. Ikeda, M. Reynolds, I. Ibáñez, J. Wang, N. Tokunaga, Y. Sasaki, H. Ohmiya, Organophotoredox-catalyzed decarboxylative N-alkylation of sulfonamides, ChemCatChem 13 (2021) 3930–3933;
(g) K. Ota, K. Nagao, D. Hata, H. Sugiyama, Y. Segawa, R. Tokunoh, T. Seki, N. Miyamoto, Y. Sasaki, H. Ohmiya, Synthesis of tertiary alkylphosphonate oligonucleotides through light-driven radical-polar crossover reactions, Nat. Commun. 14 (2023) 6856.
[15] N.J. Treat, H. Sprafke, J.W. Kramer, P.G. Clark, B.E. Barton, J. Read De Alaniz, B. P. Fors, C.J. Hawker, Metal-free atom transfer radical polymerization, J. Am. Chem. Soc. 136 (2014) 16096–16101.
[16] H. Zhou, L. Zhang, P. Wen, Y. Zhou, Y. Zhao, Q. Zhao, Y. Gu, R. Bai, M. Chen, Initiator-activation strategy-enabled organocatalyzed reversible-deactivation radical polymerization driven by light, Angew. Chem. Int. Ed. 62 (2023) e202304461.
[17] H. Ando, H. Takamura, I. Kadota, K. Tanaka, Strongly reducing helical phenothiazines as recyclable organophotoredox catalysts, Chem. Commun. 60 (2024) 4765–4768.
[18] J. Sun, Y. Wei, T. Lv, C. Wang, S. Song, J. Zhou, J. Li, Organic photoredox catalytic difluoroalkylation of unactivated olefins to access difluoro-containing tetrahydropyridazines, Org. Lett. 26 (2024), 9973–9977. 6101.
[19] (a) F. Seyfert, H.-A. Wagenknecht, N-Arylbenzo[b]phenothiazines as reducing photoredox catalysts for nucleophilic additions of alcohols to styrenes: shift towards visible light, Synlett 32 (2021) 582–586;
(b) F. Speck, D. Rombach, H.-A. Wagenknecht, N-Arylphenothiazines as strong donors for photoredox catalysis – pushing the frontiers of nucleophilic addition of alcohols to alkenes, Beilstein J. Org. Chem. 15 (2019) 52–59;
(c) D. Rombach, H. Wagenknecht, Angew. Chem. Int. Ed. 59 (2020) 300–303.
[20] N. Sugihara, Y. Nishimoto, Y. Osakada, M. Fujitsuka, M. Abe, M. Yasuda, Sequential C-F bond transformation of the difluoromethylene unit in perfluoroalkyl groups: a combination of fine-tuned phenothiazine photoredox catalyst and Lewis acid, Angew. Chem. Int. Ed. 63 (2024) e202401117.
[21] S. Jin, Dang HangT, G.C. Haug, R. He, V.D. Nguyen, V.T. Nguyen, H.D. Arman, K. S. Schanze, O.V. Larionov, Visible light-induced borylation of C–O, C–N, and C–X bonds, J. Am. Chem. Soc. 142 (2020) 1603–1613.
[22] M. Giraud, M.R. Mitha, S. Klehenz, H. Wagenknecht, N-arylphenothiazines and N, N-diarylphenazines as tailored organophotoredox catalysts for the reductive activation of alkenes, Eur. J. Org. Chem. 27 (2024) e202400847.
[23] F. Weick, N. Hagmeyer, M. Giraud, B. Dietzek-Ivanšić, H. Wagenknecht, Reductive activation of aryl chlorides by tuning the radical cation properties of *N*-phenylphenothiazines as organophotoredox catalysts, Chem. Eur. J. 29 (2023) e202302347.
[24] S. Halder, S. Mandal, A. Kundu, B. Mandal, D. Adhikari, Super-reducing behavior of benzo[b]phenothiazine anion under visible-light photoredox condition, J. Am. Chem. Soc. 145 (2023) 22403–22412.
[25] (a) J. Liu, H. Liu, X. Guo, Z. Wang, X. Wu, J. Li, C. Zhu, Green Chem. 25 (2023) 3847–3851;
(b) A. Jiménez-Almarza, A. López-Magano, R. Mas-Ballesté, J. Alemán, ACS Appl. Mater. Interfaces 14 (2022) 16258–16268;
(c) Yeonseon Ahn, Da Eun Jang, Yong-Bum Cha, Mansu Kim, Gwang-Hyeon An, Young Chul Kim, Bull. Korean Chem. Soc. 34 (2013) 107–111;
(d) S. Jana, C. Empel, C. Pei, T. Vinh Nguyen, R.M. Koenigs, Adv. Synth. Catal. 362 (2020) 5721–5727;
(e) C. Liu, Y. Shen, K. Yuan, Org. Biomol. Chem. 17 (2019) 5009–5013.
[26] Recently, phenothiazine catalyzed energy transfer reaction was reported. See; R. Hojo, K. Bergmann, S.A. Elgadi, D.M. Mayder, M.A. Emmanuel, M.S. Oderinde, Z.M. Hudson, J. Am. Chem. Soc. 145 (2023) 18366–18381.
[27] Recently, phenothiazine catalyzed photoredox catalysis via reductive quenching cycle was reported. See; J. Sun, Y. Wei, W. Wang, W. Lin, C. Wang, J. Zhou, G. Wang, J. Li, Organic photoredox catalytic sulfonylation of enaminones to access 3-sulfonyl chromones, Adv. Synth. Catal. 367 (2025) e202401396.
[28] T. Yumura, T. Nanjo, Y. Takemoto, Benzophenothiazine/boronic acid cooperative photocatalysis enables the synthesis of γ-lactones via the [3 + 2] cycloaddition of α,β-unsaturated carboxylic acids with olefins, ACS Catal. (2025) 4975–4983.
[29] (a) H. Lindner, W.M. Amberg, T. Martini, D.M. Fischer, E. Moore, E.M. Carreira, Cobalt-catalyzed photo-semipinacol rearrangement of unactivated allylic alcohols, Angew. Chem. Int. Ed. 63 (2024) e202319515;
(b) D.M. Fischer, M. Freis, W.M. Amberg, H. Lindner, E.M. Carreira, Organophotocatalytic carboheterofunctionalization of unactivated olefins with pendant nucleophiles, Chem. Sci. 14 (2023) 7256–7261;
(c) H. Lindner, E.M. Carreira, Photo- and cobalt-catalyzed cycloisomerization of unsaturated guanidines, (iso-)ureas, and carbonates, Org. Lett. 27 (2025) 704–708.
[30] H. Lindner, E.M. Carreira, Photo- and cobalt-catalyzed synthesis of heterocycles via cycloisomerization of unactivated olefins, Angew. Chem. Int. Ed. 63 (2024) e202407827.
[31] (a) I. Ghosh, T. Ghosh, J.I. Bardagi, B. König, Science 346 (2014) 725–728;
(b) I.A. MacKenzie, L. Wang, N.P.R. Onuska, O.F. Williams, K. Begam, A. M. Moran, B.D. Dunietz, D.A. Nicewicz, Nature 580 (2020) 76–80.
[32] T. Kodo, K. Nagao, H. Ohmiya, Organophotoredox-catalyzed semipinacol rearrangement via radical-polar crossover, Nat. Commun. 13 (2022) 2684.
[33] H. Wang, N.T. Jui, Catalytic defluoroalkylation of trifluoromethylaromatics with unactivated alkenes, J. Am. Chem. Soc. 140 (2018) 163–166.
[34] (a) Representative reports using cat. J see; S.R.N. Kolusu, I. Sánchez-Sordo, C. Aira-Rodríguez, E. Azzi, M. Nappi, Photocatalytic deoxygenative Z-selective olefination of aliphatic alcohols, Nat. Commun. 16 (2025) 3155;
(b) O.P. Williams, A.F. Chmiel, M. Mikhael, D.M. Bates, C.S. Yeung, Z.K. Wickens, Practical and general alcohol deoxygenation protocol, Angew. Chem. Int. Ed. 62 (2023) e202300178;
(c) K. Tagami, M. Nakayama, T. Kanbara, D. Cahard, T. Yajima, 10-Phenylphenothiazine-organophotocatalyzed bromo- perfluoroalkylation of unactivated olefins, J. Org. Chem. 89 (2024) 7084–7094;
(d) C. Yang, M.D. Kärkäs, G. Magallanes, K. Chan, C.R.J. Stephenson, Organocatalytic approach to photochemical lignin fragmentation, Org. Lett. 22 (2020) 8082–8085;
(e) P. Seefeldt, A. Villinger, M. Brasholz, Photoredox-catalyzed carbon radical generation from α-keto- N,O-acetals: synthesis of functionalized azepino[1,2-a] indoles and azepino[1,2-a]furo[3,2-b]indoles, Adv. Synth. Catal. 366 (2024) 24–30;
(f) S. Trienes, J. Xu, L. Ackermann, Photoinduced C–H arylation of 1,3-azoles via copper/photoredox dual catalysis, Chem. Sci. 15 (2024) 7293–7299;
(g) S. Li, X. Li, J.-P. Yu, X.-F. Xia, Organic photoredox catalyst induced divergent transformations of o-halogenated benzamides, Org. Chem. Front. (2025) doi: 10.1039.D5QO00407A.
[35] J. Zhang, Y. Zhang, L. Qian, Z. Zuo, Photoinduced cross-coupling of trifluoromethylarenes with heteroarenes via unactivated C(sp3)–F and C(sp2)–H selective cleavage, Org. Lett. 27 (2025) 381–385.
[36] (a) J. Xu, J.-W. Liu, R. Wang, J. Yang, K.-K. Zhao, H.-J. Xu, Construction of C–X (X = S, O, Se) Bonds via Lewis acid-promoted functionalization of trifluoromethylarenes, ACS Catal. 13 (2023) 7339–7346;
(b) S. Li, X. Li, K. Zhao, X. Yang, J. Xu, H.-J. Xu, Defluorinative haloalkylation of unactivated alkenes enabled by dual photoredox and copper catalysis, J. Organomet. Chem. 89 (2024) 13518–13529.
[37] M.H. Aukland, M. Šiaučiulis, A. West, G.J.P. Perry, D.J. Procter, Metal-free photoredox-catalyzed, formal C–H/C–H coupling of arenes enabled by interrupted pummerer activation, Nat. Catal. 3 (2020) 163–169.
[38] F.-D. Lu, D. Liu, L. Zhu, L.-Q. Lu, Q. Yang, Q.-Q. Zhou, Y. Wei, Y. Lan, W.-J. Xiao, Asymmetric propargylic radical cyanation enabled by dual organophotoredox and copper catalysis, J. Am. Chem. Soc. 141 (2019) 6167–6172.
[39] K. Targos, O.P. Williams, Z.K. Wickens, Unveiling potent photooxidation behavior of catalytic photoreductants, J. Am. Chem. Soc. 143 (2021) 4125–4132.
[40] N. Hölter, N.H. Rendel, L. Spierling, A. Kwiatkowski, R. Kleinmans, C.G. Daniliuc, O.S. Wenger, F. Glorius, Phenothiazine sulfoxides as active photocatalysts for the synthesis of γ-lactones, J. Am. Chem. Soc. 147 (2025) 12908–12916.
[41] L. Pan, A.S. Kelley, M.V. Cooke, M.M. Deckert, S. Laulhé, Transition-metal-free photoredox phosphonation of aryl C–N and C–X bonds in aqueous solvent mixtures, ACS Sustain. Chem. Eng. 10 (2022) 691–695.
[42] (a) S. Wu, J. Kaur, T.A. Karl, X. Tian, J.P. Barham, Angew. Chem. Int. Ed. 61 (2022) e202107811;
(b) B. Pfund, O.S. Wenger, JACS Au 5 (2025) 426–447;

(c) M. Lepori, S. Schmid, J.P. Barham, Beilstein J. Org. Chem. 19 (2023) 1055–1145.
[43] (a) J. Xu, J. Cao, X. Wu, H. Wang, X. Yang, X. Tang, R.W. Toh, R. Zhou, E.K. L. Yeow, J. Wu, J. Am. Chem. Soc. 143 (2021) 13266–13273;
(b) A.C. Shaikh, M.M. Hossain, J. Moutet, A. Kumar, B. Thompson, V.M. Huxter, T. L. Gianetti, Angew. Chem. Int. Ed. 64 (2025) e202420483;
(c) R.S. Shaikh, S.J.S. Düsel, B. König, ACS Catal. 6 (2016) 8410–8414;
(d) M. Neumeier, D. Sampedro, M. Májek, V.A. de la Peña O'Shea, A. Jacobi von Wangelin, R. Pérez-Ruiz, Chem. Eur. J. 24 (2018) 105–108;
(e) J.C. Herrera-Luna, D.D. Díaz, M.C. Jiménez, R. Pérez-Ruiz, ACS Appl. Mater. Interfaces 13 (2021) 48784–48794.
[44] (a) V.A. Pistritto, M.E. Schutzbach-Horton, D.A. Nicewicz, J. Am. Chem. Soc. 142 (2020) 17187–17194;
(b) M.R. El-kholany, T. Senoo, A. Mizutani, H. Takamura, T. Suzuki, I. Kadota, K. Tanaka, Org. Lett. 27 (2025) 4870–4874;
(c) G. Ju, Y. Li, Y. Zhao, Org. Biomol. Chem. 21 (2023) 6503–6508.